1

Synthesis of Siloles (and Germoles) that Exhibit the AIE Effect

Joyce Y. Corey

Department of Chemistry and Biochemistry, University of Missouri–St. Louis, USA

1.1 Introduction

As reported in 2001 by Tang and co-workers [1], the identification of the aggregation-induced emission (AIE) effect was intimately connected with a study of siloles and stemmed from the simple observation that a wet spot containing 1-methyl-1,2,3,4,5-pentaphenylsilole ($Ph_4C_4SiMePh$) (MPS) on a thin-layer chromatographic (TLC) plate barely fluoresced under UV light but was clearly visible when the spot dried. In contrast to the expectation of the time period that in the solid state aggregation would cause quenching [aggregation-caused quenching (ACQ)] of the photoluminescence (PL) processes of luminophoric molecules, the silole exhibited the reverse behavior: a sample was virtually nonfluorescent in solution but fluorescent in the solid state. For applications in electronic devices, thin films of a luminophoric material are required and the appearance of ACQ would thus inhibit such applications. An electroluminescent (EL) device was constructed with MPS and was demonstrated to be a good light-emitting material for device applications [1]. The observation of AIE in siloles was not the beginning of the search for siloles that could be efficiently incorporated into organic light-emitting diodes (OLEDs), as Tamao *et al*. had demonstrated in 1996 that siloles were efficient electron-transporting materials and showed that the device performance was related to the substituents in the 2,5-positions of the ring [2]. This was actually the first demonstration that siloles could be good candidates as core components for organic EL devices. The AIE luminogens, however, have additional applications, for example, as chemical sensors, biological probes, and smart nanomaterials. The 'turn-on/light-up' nature of an AIE sensor makes for ready use in the field or for on-sight screening, to name just a couple of applications, which will be highlighted in other chapters.

Aggregation-Induced Emission: Fundamentals, First Edition. Edited by Anjun Qin and Ben Zhong Tang.

This chapter focuses on the synthetic methods that have been used to target silacyclopentadiene and germacyclopentadiene derivatives (common names: silole and germole) and their related benzene-annulated derivatives. Synthetic examples that have actually been described as exhibiting the AIE effect will be discussed whenever possible. However, silole systems have been studied since the first report in 1959 by Braye and Hübel of the formation of $Ph_4C_4SiPh_2$ (HPS), presumably by a rather obscure synthesis from reaction of $Fe_2(CO)_6(PhC_2Ph)_2$ with Ph_2SiCl_2, and related to that which was used to produce pentaphenylphosphole from the same iron precursor and $PhPCl_2$ [3a]. The same group subsequently described a better method for the synthesis of HPS [3b] that is still in use today and is the first method that will be described in Section 1.3.1. The material covered will not provide a comprehensive listing of all systems that have been prepared but will attempt to describe the methodology that has been developed for targeting the silole core, illustrated with selected examples. Since three of the principal methods for silole formation predate the discovery of the AIE effect, testing for this phenomenon has understandably not been reported in publications prior to 2001. One of the more interesting examples was the first viable synthesis of HPS (in 1961), where it was stated: 'In the solid state it exhibits a strong blue fluorescence in ultraviolet light . . . ' [3b]. It is this solid-state fluorescence that has become a feature of the AIE effect and proves once again that 'chance favors the prepared mind' in its discovery.

The rest of this chapter is divided into the following sections. Section 1.2 contains background material on the nomenclature of siloles and their benzene-annulated relatives and the numbering systems that are commonly used and that will be utilized in this chapter. A brief introduction to the bond formation methods in silicon chemistry that are relevant to the formation of siloles will be included, as this type of chemistry imposes certain limitations on how the synthesis of a particular silole might be approached. In general, it is the role of organic chemistry in forming the carbon portion of siloles and their related derivatives that has actually enabled the presence of various substitution patterns to be incorporated into the target metallacycle. This is seen particularly in the Tamao synthesis (Section 1.3.2) of siloles and in the formation of precursors to the benzene-annulated systems (Section 1.6.2). The substitution reactions possible at both the silicon center and the carbon centers of the metallacycle also play a role, particularly in the area of copolymer synthesis. Lastly, Section 1.2 gives brief comments on the early calculations for the HOMO and LUMO energy levels for siloles as compared with the related carbon parent and the heterocycles of N and S.

Section 1.3 contains the bulk of the synthetic chemistry and describes three basic approaches to siloles as well as the more recent methodology that involves the use of transition metals both stoichiometrically (early work) and catalytically. Section 1.4 covers methods that can be used to modify the silole core and 1.5 addresses whether the synthetic methods can be extended to the heavier Group 14 element, germanium. Section 1.6 will describe basic routes to silaindenes and silafluorenes that are related to those used for siloles. Section 1.7 contains a brief discussion on the extension to oligomers and both homo- and copolymers that contain a silicon or germanium metallole, metallaindene, and metallafluorene. The last section contains a summary and commentary on future directions.

1.2 Background

The numbering scheme for siloles and the benzene-annulated derivatives is illustrated in Figure 1.1. The silaindenes are sometimes referred to as benzosiloles and the silafluorenes as dibenzosiloles, but the first name listed will be used in this chapter. The silaindene shown is technically 1*H*-1-silaindene and the silafluorene is 9*H*-9-silafluorene, but the 1*H* and 9*H* are often omitted The germanium analogs are similarly numbered and named (germaindenes and germafluorenes).

Probably the limiting factor in the assembly of the systems shown in Figure 1.1 is the small number of C—Si bond formation methods. One of the two general methods involves a salt metathesis reaction of an

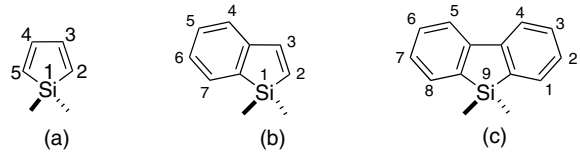

Figure 1.1 *Skeleton structures with positions numbered. (a) Siloles; (b) 1-silaindenes (benzosiloles); (c) silafluorenes (dibenzosiloles).*

organolithium or organoGrignard reagent with a silicon halide (elimination of a metal halide). The second is addition of an Si—H bond to an unsaturated organic substrate, >C=C< or —C≡C—. Such a reaction is referred to as hydrosilylation and is commonly initiated with a transition metal catalyst. Nucleophilic substitutions at silicon dominate organosilicon chemistry. From an organic chemist's perspective, organosilicon chemistry is currently a matter of manipulation of single bonds. Although compounds that contain an Si=X unit (X = C, Si, N, P, transition metal) are known, their practical use in synthesis awaits future development. An exception to these general observations is the recently published transition metal-promoted reactions that can involve SiH—HC coupling for ring closure.

Simple calculations (*ab initio*) performed for the model silole $H_4C_4SiH_2$ with a comparison with the parent carbon system, $H_4C_4CH_2$, and the sulfur heterocycle, H_4C_4S, and also a series of N heterocycles demonstrated that the silole had the lowest HOMO–LUMO energy gap in addition to a low-lying LUMO level [2, 4], The low-lying LUMO level was attributed to efficient σ^*–π^* overlap from the σ^* orbital associated with the exocyclic σ-bonded substituents on the silicon center and the π^* orbital of the butadiene unit. No such orbital is available for the parent carbon species or for the other five-membered heterocycles (with N, O or S heteroatoms). However, model systems, although simpler to calculate, do not reveal the role that substituents may play in the relative energies of the HOMO and LUMO, nor do they indicate substituent variations that might lead to better electron-transporting (ET) materials. Marder and co-workers summarized the effects of substituents on the electronic structure of siloles, including the physical data that support the trends that illustrate the importance of substituents and their location on the silole core [5]. Yamaguchi and Tamao also briefly reviewed the role of orbital interactions in main group element-containing π-electron systems, heteroles, dibenzoheteroles, and element-bridged stilbenes, although the focus was on boron and silicon heteroatoms [6].

Although the synthesis reported for HPS in 1961 [3b] is still in use today, other approaches have been developed especially since the 1990s. What becomes useful to an individual investigator will depend on the substitution pattern desired either on the carbon backbone or the silicon center. Two fundamental strategies are possible, one in which the carbon core is constructed and then connected to the heteroatom, and the other where the substituents are added to the silicon center and then C—C bond formation between two of the substituents is initiated. In either case, a common precursor will be an alkyne or diyne even when the C—C bond is formed between two of the silicon substituents. Transition metal-catalyzed formation of siloles (and their benzene-annulated derivatives) is of relatively recent origin and the actual ring formation details will vary depending on the catalyst. As will be seen, the most commonly prepared siloles have substituents on all (four) carbons, but this will not be the case for either silaindenes or silafluorenes. In fact, methods to obtain substituted precursors to silafluorenes are actually relatively recent. In Section 1.3 the synthetic methods will be introduced in the following order: Section 1.3.1, reductive dimerization of 1,2-diarylalkynes; Section 1.3.2, intramolecular reductive cyclization of dialkynylsilanes; Section 1.3.3, 1,1-organoboration of dialkynylsilanes; and Section 1.3.4, transition metals in silole formation. Modifications that utilize preformed siloles to include a desired C or Si substituent are the subject of Section 1.4.

1.3 Synthesis of Siloles

There have been several general reviews of the synthesis of main group heterocycles or heterocycles of silicon (with varying ring sizes) [7] and others that involve only siloles and related compounds [8]. Additional reviews that are more narrowly focused will be mentioned where the particular synthetic method is described.

1.3.1 Reductive dimerization of tolan

Historically, the first practical method for the formation of siloles involved a ring closure at a silicon center by a metathesis reaction of a dilithio reagent generated from Li and PhC≡CPh (tolan) with Ph_2SiCl_2 to give HPS in 50% yield. Subsequently, this synthetic approach has often been referred to as the Curtis method (Equation 1.1).

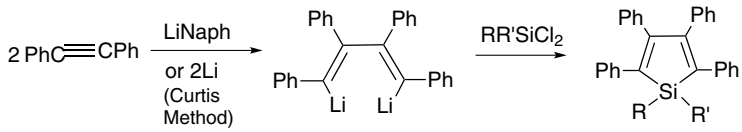

(1.1)

The reductive dimerization of tolan (diphenylacetylene) with Li metal or LiNaph (lithium naphthalenide) results from the transfer of an electron to PhC_2Ph to produce a radical anion that dimerizes to give the dianion, 1,4-dilithio-1,2,3,4-tetraphenylbutadiene [9a]. An ethereal solution from the reaction of Li and PhC_2Ph develops a deep red color and deposits a red precipitate, which, when quenched with water, gives 1,2,3,4-tetraphenylbutadiene. However, if the solution turned brown (with a brown precipitate), aqueous quenching provided 1,2,3-triphenylnaphthalene and seemed to occur when excess metal was present [9a]. The color change signifies 'death' from the standpoint of the potential generation of a silole and, unfortunately, the trigger for this catastrophic rearrangement is unknown. Braye *et al.* commented on the problem in the first practical synthesis of HPS and suggested that the reaction time should be limited and that working on a larger scale could suppress the rearrangement [3b]. In contrast to early recommendations that the stoichiometry for the reaction of PhC≡CPh with Li (or LiNaph) be held at 1:2, various investigators have used acetylene-to-Li ratios ranging from 0.2:1 to 2:1 and have achieved modest yields that generally lay between 40 and 70% after reaction with an appropriate chlorosilane [8c]. A variety of dichlorosilanes have been used as the quenching agent, including the types R_2SiCl_2 (such as R = Ph, Me), $RR'SiCl_2$ (R,R′ = PhMe), and also the chlorosilanes $HSiCl_3$ and $SiCl_4$. With $HSiCl_3$, the silole produced is Ph_4C_4SiHCl, which has two functional groups on silicon that can be substituted by different types of reactions: salt metathesis of Si—Cl to incorporate mainly an organic substituent and hydrosilylation of multiple bonds with HSi. With $SiCl_4$, the product is $Ph_4C_4SiCl_2$. One of the more interesting tactics in trying to control the degradation of the dilithiobutadiene was through monitoring the reaction for the presence of butadiene in hydrolyzed aliquots of the reaction mixture by gas chromatography (GC), then freezing in liquid N_2. In this case, the $SiCl_4$ is layered over the solidified reaction mixture, then warmed slowly to room temperature. The yield of isolated $Ph_4C_4SiCl_2$ was 50–70% [9b,c], Because the range of commercially available dichlorosilanes is not large, $Ph_4C_4SiCl_2$ is often generated *in situ* and then treated with organometallic reagents such as $LiC_6H_4CH_2NEt_2$-*p* [10], C_6F_5MgBr [11], and several other cases listed in [8c]. This same tactic of generating the functional silole *in situ* by quenching with $HSiCl_3$ followed by an organometallic reagent has also provided several examples of Ph_4C_4SiHR [8c].

The reductive dimerization of ArC≡CAr has almost exclusively been performed for Ar = Ph, although there is one example where Ar = 9,9-dimethylfluoren-2-yl [12]. It is certainly likely that substituted

aromatic rings such as $-C_6H_4X$ (X in a *meta* or *para* position) could be utilized, but such experiments do not seem to have been reported in the literature. The reductive dimerization of PhC≡CAr is more problematic as three silole isomers could be formed: 2,4-diphenyl, 2,5-diphenyl, and 3,4-diphenylsilole. One of the more interesting cases reported recently was the reaction utilizing PhC≡CAr, Ar = 2,6-diisopropylphenyl, where the $silole_{2,4}$:$silole_{2,5}$:$silole_{3,4}$ ratio was found to be 40:2.3:1, with the most sterically hindered silole (i.e. with the two diisopropylphenyl substituents on adjacent positions) formed in the least amount. In what must be a real *tour de force* effort, the three isomers were isolated after 20 chromatographic separations [13]. Calculations were reported for $C_4Ph_4SiMe_2$ and $C_4Ph_2Ar_2SiMe_2$ [Ar = 3,4-bis(2,6-diisopropylphenyl)] about a year later [14]. The calculations showed that the twisting motions of the phenyl groups in the 3,4-positions dissipate the excited-state energy nonradiatively. The presence of the bulky 2,6-diisopropyl groups on the phenyl rings in the 3,4-positions completely suppressed this channel for loss of energy, resulting in enhanced PL [14].

Although the AIE effect was first identified in 2001 [15] by Tang and co-workers during a study of the properties 1-methyl-1,2,3,4,5-pentaphenylsilole (MPPS), it could just as well have been HPS that was the subject of a report by Tang's group published about a month later [16]. Historically it is HPS that was the first silole that was reported and has subsequently become a 'poster child' for silole chemistry. HPS has been widely studied since the end of the 1990s in terms of physical measurements that have been reported in at least 15 publications (about half of which are from Tang's group). Three papers contain synthetic details, with minor experimental differences, for the preparation of HPS utilizing PhC≡CPh and Li followed by addition of Ph_2SiCl_2 (PhC≡CPh:Li, %: 1:1, 44% [17]; 1:2, 68% [16]; 1.05:1, 60% [18]), and all give spectroscopic data including PL measurements and activation energies. The X-ray structure has also been determined [19, 20], Electrochemical properties have been reported for HPS from cyclic voltammetric (CV) measurements [17] and also photoelectron spectroscopy (PES) and inverse photoelectron spectroscopy (IPES) data, including density functional theory (DFT) calculations. Calculations have also been reported including equilibrium geometries (MO) [17], excitation energies [time-dependent density functional theory (TD-DFT)] [21], excited-state properties (DFT methods) [22], carrier transport properties (Hartree-Fock and DFT) [23] and calculated structures to compare with experimental structures (DFT Dmol3 package) [24]. Electron mobility in films has been measured and that of the HPS was ∼1.5 times higher than that of an MPPS film, hence it has better ET properties in a light-emitting diode (LED). HPS also has a higher mobility than that of Alq_3 [tris(8-hydroxyquinolinato)aluminum], a widely used electron transport material [24].

A desirable feature for an OLED device is a high PL quantum yield (Φ_{PL}) in the solid state. The quantum yield for various siloles has certainly been reported, but at this point only the results for HPS will be described. The value of Φ_{PL} is determined by comparison with a standard, although the choice of standard is not uniform for all studies. The solution Φ_{PL} is a function of the solvent and, for solids, the particular phase (different solid forms). The solution Φ_{PL} has been measured in six solvents (in the same study) with values that are low in all five solvents in which HPS is soluble (insoluble in EtOH) and follows the order dioxane > C_6H_6 > THF > CH_2Cl_2 > CH_3CN, with values varying from 0.42 to 0.09% [20]. The Φ_{PL} values for HPS as an average over the solvents was 0.21%, for the solution aggregates from dioxane–water 38% and for an SOA (sucrose octaacetate) glass containing HPS 59% [20]. The enhancement of the value of Φ_{PL} of HPS on SOA glass over its solution value in dioxane was 140-fold.

The Φ_{PL} for HPS crystalline films, amorphous films, and nanowires with various diameters has been reported with accompanying time-dependent fluorescence measurements. The results indicate that the excited states of HPS decay through a fast and a slow pathway. In crystalline HPS (Φ_{PL} = 86%), 94% of the molecules decay through a slow pathway (6% by the fast pathway). In the amorphous form (Φ_{PL} = 78%), 75% of the molecules decay by the slower pathway. The nanowires decay by an increasing extent through the faster pathway as the diameter of the nanowire increases in increments from 35 nm (14%) to 250 nm

(21%). It was concluded that the fast-pathway decay contributes little to the emission spectra whereas the relaxation of the excited states dominates the slower deactivation process [25]. In another study, the Φ_{PL} value for HPS was determined in cyclohexane to be 0.30% and in a thin film 78%, which is a 260-fold enhancement from solution to the solid, and with the corresponding $Ph_4C_4SiPhMe$ that enhancement was 654-fold [24].

When a silole is dissolved in a 'good' solvent, PL is very weak. However, once a large amount of water (a 'poor' solvent) is added, intense PL spectra are obtained. The siloles aggregate with higher water content, and since there is no observable precipitate, nanoparticles were suspected to be the source of the PL [15]. The size distribution of the nanoparticles formed from HPS in water–acetone mixtures at 70 and 90% volume fractions of water exhibited average particle sizes of $\sim$53 and $\sim$82 nm, respectively. In this study, the AIE effect (enhanced emission in the solid state) was attributed to restricted intramolecular rotation (RIR) of the phenyl rotors around the single bonds that link them to the core of the silole [19].

The AIE effect for nanoparticles has been explored in several applications, a few of which are described here. A ball-milling process was used to obtain nanocrystalline HPS, which was encapsulated in thin polyelectrolyte layers that then provided an 'interface' for the attachment of antibodies through adsorption at the interface. The usual quenching problem arising for the ratio of fluorescent dyes to biomolecules (F:P ratio $= 2.4 \times 10^{-3}$) is prevented by the AIE property of the silole. The fluorescence signal from the nanocrystalline siloles was 40–140-fold higher in an M IgG assay compared with direct FITC-labeled antibodies [26]. The isolation of HPS nanostructures from THF by addition of water along with attendant (SEM) images for those isolated from 60, 70, 80, and 90% water illustrated the changes in morphology of the nanoparticles and included nanoflowers at 70% water, nanoglobules mixed with nanoflowers at 80% and microglobules at 90%. The various types exhibited enhanced and color-tunable photophysical properties. The nanoflowers produced in 70% water in THF exhibited a 100-fold increase in intensity relative to the emission for dilute THF solutions. Time-resolved fluorescence data gave a mean lifetime of 4.6 ns for the nanoflowers and a fluorescence quantum efficiency of 35% [27]. Nanowires of HPS with tunable PL have also been reported when nanoporous alumina membranes were immersed in a saturated solution of the silole. Nanowires with different diameters were observed and characterized, in part, by SEM images and also by X-ray diffraction (XRD). HPS aggregates have also been incorporated into a chitosan film where the fluorescence emission is stable and selective for the presence of picric acid with a detection limit of $\sim 2 \times 10^{-8}$ mol l^{-1}. Related compounds such as trinitrotoluene (TNT), dinitrotoluene (DNT), and nitrobenzene (and others) had no effect on the fluorescence emission of the field [18].

The vapochromism of HPS absorbed on a TLC plate was reported since a sample of HPS fluoresces when dry but not when exposed to solvent vapor, and this 'off' and 'on' behavior was reversible. If the film is formed on a quartz surface, a change from a green fluorophore to a blue emitter takes place after exposure to solvent and is not reversible. The SEM and TEM images of the film before and after exposure to acetone clearly show a transformation from an amorphous phase (before) to a crystalline phase (after) [28]. In a similar type of experiment, HPS thin films were prepared by spin coating and subjected to solvent fuming and the results of solvent annealing were monitored by SEM images. When the film was subjected to methanol annealing, nanobelts, and nanorods were observed, but after benzene vapor annealing the nanoparticles disappeared and an amorphous HPS film was observed. Annealing with isopropyl alcohol vapor followed by chlorobenzene vapor annealing revealed the same sequence as did acetone vapor annealing followed by THF vapor annealing. The SEM images provide convincing evidence for the crystal formation [29]. Although SEM images may be the most helpful in determining morphologies of crystalline solids, there is some support for the use of Fourier transform infrared (FTIR) spectra in demonstrating crystal powders versus amorphous powders, although this was demonstrated not for HPS but for 1,1-bis(2′-thienyl)-2,3,4,5-tetraphenylsilole [30].

The previous paragraph gives only a hint of the applications of the AIE effect in siloles. There are siloles that are prepared by other methods, primarily the Tamao procedure (covered in the next section), and by

appropriate substitution reactions at silicon (described in Section 1.4.1). For a more extensive discussion of applications that include siloles, see the reviews on luminogenic materials with AIE [31a], a brief account of the Tang group's development of the AIE mechanism and applications [31b], and AIE in both silole molecules and polymers where other researchers' efforts are included [31c].

Before leaving this section, the strengths and weaknesses of the Curtis method should be mentioned. The reaction involves the use of tolan, a commercially available material that automatically places phenyl substituents on each of the carbon atoms of the silole core. The reaction is not practical for unsymmetrically substituted alkynes (ArC≡CAr′) as three silole isomers can form, and it also cannot be used for alkynes with alkyl or silyl substituents (these will be incorporated later in another method). The synthetic approach can be used to ring close at silicon with a variety of chlorosilanes with two or more Cl substituents. Although the carbon core substituents are not varied, those at the silicon center (1,1-position) are readily varied through standard nucleophilic substitutions of an SiCl bond or reaction of an SiH bond with a multiple bond. The next section describes the synthesis of siloles where the 2,5-substituents may differ from the 3,4-substituents.

1.3.2 Intramolecular cyclization of dialkynylsilanes

A completely new approach to silole formation was introduced by Tamao and co-workers in 1994. In this method, two alkynyl groups tethered to silicon are cyclized by reductive coupling of two carbon centers using LiNaph (or Li) as the reductant. The ring closure reaction places two anionic centers on the carbons α to the Si center, thus permitting the introduction of substituents either through salt metathesis with a silicon halide or ultimately by a cross-coupling reaction (Equation 1.2). Yamaguchi and Tamao summarized the early work on this new silole-forming method [32] and on the role of cross-coupling of silole monomers in oligomer and polymer formation [33].

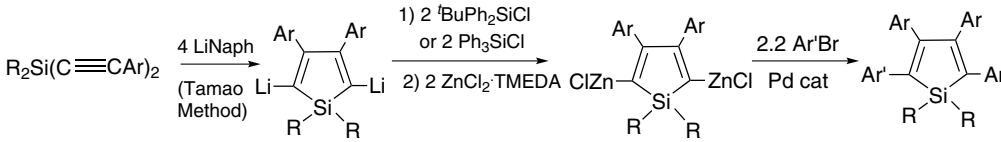

(1.2)

The Tamao 'one-pot' approach to siloles has become the most popular method for the generation of siloles, although it does require the synthesis of the appropriate dialkynylsilane precursors as these are not commercially available. Although some details of the method appeared in a paper on oligosiloles [34a] in 1994, a full paper describing the procedure for monomeric siloles was not published until 2000 and provided the details for the isolation of 17 siloles from $Me_2Si(C{\equiv}CPh)_2$ [34b]. The reaction method requires simultaneous reduction of the carbon atoms of the alkyne β to the Si center followed by the coupling of the two radical centers to form a C—C bond and closing the ring. Not surprisingly, an aryl substituent is required on the β-carbon, as the precursors such as $R_2Si(C{\equiv}CR')_2$ where R′ = alkyl or silyl give complex mixtures of products from the reduction. Although the intermediate dilithiosilole that is formed can be quenched with a simple reagent such as MeI [35], the more common route is to treat the dilithiosilole with $ZnCl_2$ (or $ZnCl_2$·tmeda) to form the 2,5-ZnCl-substituted silole *in situ*, which is then cross-coupled with an aromatic bromide utilizing $Pd(PPh_3)_4$ or $PdCl_2(PPh_3)_2$ as the catalyst. A second cross-coupling route utilizes the reaction of the 2,5-ZnCl substituents with Br_2 or *N*-bromosuccinimide (NBS) to give a 2,5-dibromosilole, which may or may not be isolated [36]. Isolation of three dibromides with different sets of substituents at the 1,1-position (Me_2, MePh, Ph_2) [37] was recently reported and earlier, isolation of three dibromides of $Ph_2Br_2C_4SiR_2$ where R = Et, ^{i}Pr, Hex was described [34a]. A very detailed account of the

preparation of 2,5-dibromo-1,1-dimethyl-3,4-diphenyl-1*H*-silole was published in *Organic Synthesis* [38]. The 2,5-dibromosilole is useful for cross-coupling reactions (particularly with terminal alkynes [37, 39]). Reaction conditions for the lithiation of one of the two bromides to give the intermediate monolithio intermediate ($Ph_2BrLiC_4SiEt_2$) was reported by Tamao *et al.* [34a]. Quenching of the lithio reagent with $ClSnBu_3$ gave $Ph_2Br(SnBu_3)SiEt_2$ and thus produced a silole that has two different groups that can react under different cross-coupling conditions [34a]. A second variation, reported by Pagenkopf and co-workers, was the treatment of the 2,5-dilithiosilole intermediate with *N*-chlorophthalimide followed by iodine, which provided the asymmetrically substituted 2-chloro-5-iodosilole [39]. This also then allows two different cross-coupling reactions to be performed, leading to two different substituents at the 2,5-positions, and was exploited by Pagenkopf and co-workers to introduce an electron-donating substituent at one of the positions and an electron-accepting substituent at the remaining position [39]. A listing of siloles prepared by the Tamao procedure can be found in [8c]. An important feature in the improvement of the yields for this method was the addition of a bulky silane (Ph_3SiCl) or excess $ZnCl_2$·tmeda (4 equivalents) to the intermediate dilithiosilole to quench any excess LiNaph used for the reductive coupling step [34b].

In contrast to the Curtis method (Section 1.3.1), the original Tamao procedure could not be used for silole precursors such as $Cl_2Si(C{\equiv}CPh)_2$. However, a route to mono- and difunctional siloles was developed utilizing $(Et_2N)_2SiCl_2$ (formed from $SiCl_4$ and 2 molar equivalents each of Et_2NH and Et_3N) to obtain the precursor, $(Et_2N)_2Si(C{\equiv}CPh)_2$ [40]. The successful conditions for the reductive coupling involved addition of the diethynylsilane to an excess of LiNaph at −78 °C to form the 2,5-dilithio-1,1-diaminosilole. Trapping with Me_3SiCl or dimethyl sulfate gave the 2,5-bis(trimethylsilyl)- and 2,5-dimethylsiloles in 83 and 70% isolated yields, respectively [40]. Both Et_2N– groups of both siloles could be converted to a difunctional silole with alkoxy or chloro groups. The latter conversion is an indirect route to dichlorosiloles, which could then be converted to a variety of 1,1-diorganosiloles as also described in Section 1.3.1. It should be noted that all the siloles with 2,5-methyl substituents were unstable in air.

There are many examples of different substituents that have been incorporated into the 2,5-positions and a few examples are shown in Figure 1.2. After the demonstration by Tamao's group that siloles could function as core components in ET materials, including systems where the 2,5-aryl groups have been modified, various research groups have tried to improve the quantum yields of the siloles and to obtain a range of colors from the emission (see [8c] for the variations). Just as the siloles prepared by the Curtis method were weak emitters in solution, so also are the various siloles prepared by the Tamao procedure. In an earlier review of the effects of substituent locations on the electronic structure of the siloles by Marder and co-workers [5], it was argued that the largest effects were exerted by the 2,5-substituents and that these have the greatest potential to alter the optical properties, especially if there are strong π-interactions of the substituents with the silole core [5]. Since in applications in electronic devices the silole is in the solid phase, it is the measurement of the quantum yield associated with the solid (especially thin films) that would be the most meaningful, but it is the parameter that has been least reported relative to solution quantum yields. Even at that, the quantum yield values for amorphous solids, crystalline solids and thin films can vary. For the substituents shown in Figure 1.2, quantum yields in solution were generally reported but thin-film values were reported only for PyPySPyPy (28%) [41c], PPSPP (∼62%) [41d], and the anthracenyl-substituted phenyl (which was 2.3 times the relative solid-state Φ_{PL} of DMPPS [41f]).

Several attempts have been made to molecularly engineer higher Φ_{PL} values and a few of the more recent reports are outlined here. Three publications concerning terminally substituted 2,5-alkynyl groups demonstrate how Φ_{PL} values of amorphous powders compare with the corresponding 2,3,4,5-tetraphenylsiloles although these were measured as thin films: $Ph_4C_4SiMe_2$ (73%), $Ph_4C_4SiMePh$ (95%), and $Ph_4C_4SiPh_2$ (94%)] [24]. There were three series of 2,5-dialkynylsiloles and each series included the following substituents on silicon: Ph_2, MePh, and Me_2. Within each of the three series, the highest Φ_{PL} values (measured for amorphous solids) were found for the $Ph_2(R_3SiC{\equiv}C)_2C_4SiMePh$ derivative [R = Me (33.3%), Et (76.4%),

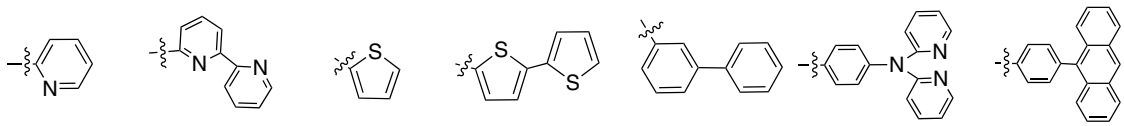

Figure 1.2 *Selected examples of substituents incorporated at the 2,5-position using the Tamao procedure starting from $Me_2Si(C{\equiv}CPh)_2$.*

^{i}Pr (99.9%)]. As the bulk of the R group in the silole increased the λ_{em} was blue shifted [42]. A later study of the same series as thin films but with $Ph_3SiC{\equiv}C-$ substituents gave lower Φ_{PL} values of 18.1% ($SiPh_2$), 28.3% (SiPhMe), and 34.6% ($SiMe_2$), the reverse of the order reported in the previous study by Tang's group [43]. An earlier study with a more complex 2,5-alkynyl substituent with phenyleneethynylene strands with up to three aromatic rings and a total of three alkynes also provided quantum yields for the solid state, but the values were less that 15% (the solid-state form was not specified) [44]. Another study included phenylacetylene dendrimers but these did not exhibit an AIE effect [45].

Other modifications with related sets of substituents have been described. In one study of various *p*-tolyl-substituted siloles, 1,1-dimethyl-2,5-bis(*p*-tolyl)-3,4-diphenylsilole, 1,1-dimethyl-2,5-diphenyl-3,4-bis(*p*-tolyl)silole, and 1,1-dimethyl-2,3,4,5-tetra(*p*-tolyl)silole were all prepared by the Tamao procedure for comparison with 1,1-dimethyl-2,3,4,5-tetraphenylsilole (DMTS). The maximum AIE enhancement was found for H_2O–THF (95:5) and decreased in the order DMTS > 3,4-bis(*p*-tolyl) > 2,3,4,5-tetra(*p*-tolyl) > 2,5-bis (*p*-tolyl). The Me group is weakly electron donating and substitution results in a small bathochromic shift in absorbance maxima and a slight enhancement of luminescence quantum yields in the 2,5-substituted case versus the 3,4-substituted silole (consistent with the earlier summary by Marder and co-workers [5]) [46]. Another study involved the *core* structure of PyPySPyPy (see Figure 1.2) where the silicon center became part of a second ring (spirocycle) with five-membered (Cy5) and six-membered (Cy6) rings. The thin-film quantum yields for these spirocycles, compared with PyPySPyPy, which has two exocyclic methyl groups ($\Phi_{PL} = 28\%$), were only slightly higher for Cy5 (30%) and Cy6 (31%) [47a]. In a related study with 2,3,3′,4,4′-hexaphenyl-1,1′-spirobisilole, the Φ_{PL} exhibited by the thin film was $55 \pm 5\%$, measured relative to Alq_3 (32%), although emission in solution was very weak ($\Phi_{PL} = 0.05\%$), consistent with the AIE effect [47b]. The Φ_{PL} values for solution (THF), aggregates (1:9 THF–water) and film have been reported to determine the effect of electron-accepting [$-C_6H_4CH{=}C(CN)_2$] substituents versus electron-donating substituents [$-C_6H_4N(Ph)_2$]. The values of $\Phi_{PL(soln)}$, $\Phi_{PL(aggr)}$, and $\Phi_{PL(film)}$ were 0.2, 11.1, and 54.1%, respectively, for the electron-accepting group and 3.2, 44.1, and 74.0%, respectively, for the electron-donating group. These values show that not only is the form of the solid state important to use in comparisons but also electron-donating substituents provide higher Φ_{PL} values [48].

Under what conditions does a quenching reaction at the 2,5-positions in the Tamao procedure give unexpected products? An interesting case is the intended preparation of 2,5-bis(dimethylsilyl)-1,1-dimethyl-3,4-diphenylsilole. Quenching the dilithio intermediate with Me_2SiHCl gave not only the desired product in 48% yield but also an unexpected 3-silolene, 2,2,5,5-tetrakis(dimethylsilyl)-1,1-dimethyl-3,4-diphenyl-3-silolene (10%) resulting from further reduction. When the exocyclic substituents at silicon were either PhMe or Ph_2, the silolene did not form. The latter results were attributed to steric hindrance at silicon [49a]. In another case, also attributed to steric hindrance probably due to the four phenyl groups (two at the silicon center), the attempt to cross-couple the intermediate $Ph_2(ClZn)_2C_4SiPh_2$ with a brominated tetraphenylethylene [catalyzed by $Pd(PPh_3)_2Cl_2$] resulted in homocoupling of the tetraphenylethylene to give 4,4′-bis(1,2,2-triphenylvinyl)biphenyl and no cross-coupling product [49b]. However, when a similar

reaction was conducted with one of the exocyclic phenyl substituents replaced by methyl, the targeted silole, 2,5-BTPEMTPS (prepared by the Tamao procedure, 35%) was isolated in 41% yield. 3,4-BTPEMTPS (35% yield) was also prepared using the Tamao procedure [49c]. The extent of the emission enhancement of the AIE effect can be related to the ratio of Φ_{aggr} to Φ_{soln}, that is, $\alpha_{AIE} = \Phi_{aggr}/\Phi_{soln}$. For 2,5-BTPEMTPS, $\Phi_{soln} = 0.34\%$ and $\Phi_{film} = 51.2\%$, whereas for 3,4-BTPEMTPS, $\Phi_{soln} = 0.38\%$ and $\Phi_{film} = 46.9\%$, giving an α_{AIE} of 150.6 for the 2,5-isomer and 123.4 for the 3,4-isomer. The corresponding α_{AIE} values for HPS and MePPS were 780 and 944. The differences between the two systems can be attributed to the presence of very bulky substituents for BTPEMTPS, which makes the phenyl rotors less free to undergo intramolecular rotations and therefore the Φ_{soln} values are higher than those of the 'parent' MPPS (or HPS). This consequently leads to a smaller value of α_{AIE} [49c]. However, the emission of the 2,5-isomer in both solution and aggregate states is more efficient than that of the 3,4-isomer, and the 2,5-isomer is electronically more conjugated (reflected in the greater red shift for the λ_{max} observed) than the 3,4-isomer [49c].

The Tamao procedure overcomes one of the inadequacies of the Curtis method in that it allows for the placement of substituents at the 2,5-positions that differ from those at the 3,4-positions (most often the 3,4-substituents are phenyl groups). This then allows for better electronic tuning, which has been shown to be most effective from the 2,5-positions. In addition, it is possible to incorporate selectively different substituents at each of these positions, thus allowing for incorporation of both electron-withdrawing and electron-donating substituents on the silole ring. The reactions at the 2,5-positions can be prone to steric hindrance to coupling, in which case reducing the bulk of the exocyclic substituents at silicon can alleviate this problem [49b,c]. An interesting, but not well-known, side aspect in the Tamao procedure is that copper-stabilized lithium cannot be used in the preparation of LiNaph as the reaction mixtures after addition of the LiNaph to the dialkynylsilane produce a gel and no silole product is observed. It is probable that the presence of copper promotes a different and unproductive reduction of the silole precursor, although this has not been verified. A limitation of the Tamao procedure is that the dialkynylsilane $R_2Si(C{\equiv}CAr)_2$ must have an aryl substituent that terminates the acetylene for a successful reductive coupling reaction. This restriction is removed in the Wrackmeyer approach, also involving dialkynylsilane precursors and which is described in the next section.

1.3.3 Intramolecular cyclization of dialkynylsilanes utilizing borane reagents

About a year before the Tamao reaction was introduced, the cyclization of $R_2Si(C{\equiv}CR')_2$ was introduced by Wrackmeyer and co-workers [50]. The overall reaction is shown in Equation 1.3 and has been proposed to occur in a two-step sequence involving 1,1-ethylboration followed by a 1,1-alkenylboration that provides the silole ring system. A unique feature of this ring closure method is that the terminal alkyne substituents are incorporated into the silole in the 2,5-positions. The early work on the 1,1-organoboration of alkynylsilicon compounds has been reviewed by Wrackmeyer [51].

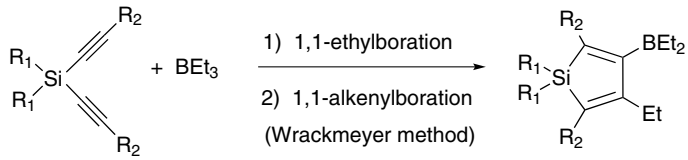

(1.3)

In the majority of the publications on the generation of siloles by Wrackmeyer and co-workers, the products were characterized spectroscopically even when solvents were removed from the product mixtures to give oils. A variety of alkylboranes were used in the Wrackmeyer procedure, including R_3B with R = allyl

[52a], boraadamantane [52b], Et [52c–e], Ph [52f], and 9-borabicyclo[3.3.1]nonane (9-BBN) [52g]. There are two ways to protodeborylate the silole with acetic acid: one is to precipitate the bicyclic boron–oxygen by-product at low temperatures and the other is to sublime out the boron–oxygen by-product under reduced pressure [53a]. Another method that removes the BR_2 substituent involved the use of ethanolamine [50]. Unlike the Tamao procedure, the BR_3-catalyzed route to siloles is compatible with SiH and SiCl bonds in the starting dialkynylsilane

The products produced in the Wrackmeyer procedure tend to decompose during distillation or chromatographic procedures, which makes them less attractive targets for silole synthesis. Only in a few rare cases were solids isolated. Erker and co-workers extended the 1,1-organoboration method to the use of $B(C_6F_5)_3$ and successfully isolated solid products from the reaction of both $Me_2Si(C{\equiv}CPh)_2$ and $Ph_2Si(C{\equiv}CSiMe_3)_2$ with $B(C_6F_5)_3$ (see Equation 1.4) and obtained X-ray structures of both [54a]. The product shown in Equation 1.4 exhibited hindered rotation about the $C{-}B(C_6F_5)_2$ bond at room temperature and this is most likely due to steric congestion between the $SiMe_3$ groups and the $B(C_6F_5)_2$ substituents. The variable-temperature ^{19}F NMR spectra provided the thermodynamic parameters for this hindered rotation [54a]. Although the fluorescence of both compounds was discussed, no determination of an AIE effect was described. A unique rearrangement of the first product is promoted by photolysis resulting in migration of the $-B(C_6F_5)_2$ substituent to the position α to the silicon center (Equation 1.4) [54b]. The borane $HB(C_6F_5)_2$ also gave the analog of the first product in Equation 1.4 (with the C_6F_5 replaced with H) and the photolysis reaction also gave the rearrangement product [54b]. In a subsequent publication, it was shown that when the reaction of $R_2Si(C{\equiv}CSiMe_3)_2$ with $HB(C_6F_5)_2$ was run at low temperatures (kinetic control), silacyclobutene products were formed, which rearranged on warming to the siloles [54c]. Erker and co-workers also demonstrated that 1,1-carboration is effective for the formation of phospholes [54d]. However, another interesting aspect of this particular report was the successful cross-coupling of the $-B(C_6F_5)_2$ substituent of the phosphole to introduce a phenyl substituent. This tactic has not been used to remove and substitute the $-B(C_6F_5)_2$ in siloles but it would probably be effective.

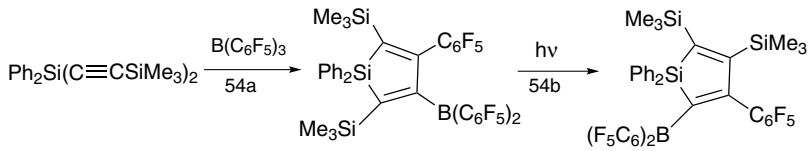

(1.4)

The acid-catalyzed approach to (monomeric) silole formation is probably best used when Me_3Si- or alkyl groups are desired in a position α to the silicon center. The importance of Me_3Si- groups is that they can be replaced with Br substituents through reaction with NBS or Br_2. The importance of bromines in this position is more clearly obvious for the incorporation of a silole unit into polymer systems, as will be described in Section 1.7. In terms of isolation of solid silole products, it is likely that the use of BPh_3 [52f] or of $B(C_6F_5)_3$ [54a] will provide products that can be purified by standard methods and subsequently characterized. The potential then is that the boryl group can be substituted by cross-coupling methods to give two different aryl substituents in the 3,4-positions of the silole, which is not easily done by any other method. It is the presence of two aryl rotors in the 3,4-positions that appears to be important for the observation of the AIE effect. The Wrackmeyer approach has been utilized for precursors with two different alkynyl groups but not of the type $R_2Si(C{\equiv}CAr)(C{\equiv}CAr')$ [52h]. However, in such a case two isomeric siloles would be formed, which would necessitate separation of the products.

1.3.4 Synthesis of siloles using transition metal reagents

Transition metals have been used stoichiometrically as precursors to siloles and also as catalysts to promote ring formation. The stoichiometric processes (Section 1.3.4.1) involve Group 4 metals and are used synthetically in two ways: (1) as a route to 1,4-dihalo-1,4-butadienes (both Zr and Ti) and (2) for exchange reactions (Zr). The catalytic methods (Section 1.3.4.2) require a preassembly of a suitable silane where the substituents on silicon are ring closed primarily by transition metal complexes.

1.3.4.1 Stoichiometric Reactions

1.3.4.1.1 Formation of 1,4-Dihalo-1,4-butadienes The reductive dimerization of tolan (the starting material for the Curtis method) in the presence of the intermediate [Cp_2Zr], formed from Cp_2ZrCl_2 and ^{n}BuLi to give $Ph_4C_4ZrCp_2$, was first reported in the mid-1980s by Negishi *et al.* [55a]. Reaction of the zirconacycle with I_2 gives 1,4-diiodo-1,2,3,4-tetraphenylbutadiene. In contrast to the reductive dimerization of tolan, the reaction through zirconium is not restricted to aryl-substituted alkynes and can be used effectively for the reaction of RC≡CR to give $R_4C_4ZrCp_2$ (e.g. R = Et) and then to $Et_4C_4I_2$ [55b,c], and also the reaction of unsymmetrically substituted alkynes such as $Me_3SiC{\equiv}CMe$, which gives 1,1-diiodo-2,3-dimethyl-1,4-bis(trimethylsilyl)butadiene upon iodination [55d]. In a related method, Buchwald and co-workers reported a variety of 1,4-diiodo-1,3-dienes by the sequential treatment of Cp_2ZrHCl with $R^1C{\equiv}CR^2$ followed by MeMgBr or MeLi (low temperature), which loses CH_4 at room temperature to give the zirconacyclopropene [55e]. Treatment with a second alkyne $R^3C{\equiv}CR^4$ results in insertion into a Zr—C bond to give the zirconacycle. However, a single regioisomer is not always observed. Cleavage of the resultant zirconacycle with I_2 gives $IR^1C{=}CR^2{-}CR^3{=}CR^4I$. Addition of 1 equiv. of CuCl in the iodination step was reported to give a significant increase in the yield to >90% for the diiodobutadiene [55f]. A novel twist on the reaction occurred when 0.5 equiv. of 'Cp_2Zr' was reacted with $R_2Si(C{\equiv}CR')_2$ (R= Ph, Me; R′ = Ph or alkyl; the same type of precursor used in both the Tamao and Wrackmeyer procedures) provided, after iodination, 1,4-diiodo-1,4-bis{(RC≡C)Me_2Si}$_2$-3,4-R'_2-butadiene [56]. Two reviews described butadiene building blocks and the synthetic applications of 1,4-dilithio-1,3-dienes [57a,b].

A second approach to 1,4-dihalobutadienes from alkynes is the one-pot procedure that is based on the commercial reagents $Ti(OPr^i)_4$ and ^{i}PrMgCl [probably generates $(^i PrO)_2Ti(\eta^2$-propene)]. Reaction with a dialkyne, RC≡C—CH_2—X—CH_2C≡CR (R varies; X = $(CH_2)_n$, n = 0, 1, 2), or an alkyne, RC≡CR′ (R = Me or H, R′ = Ph, $SiMe_3$), which then forms a titanacyclopentadiene. Halogenation provides the 1,4-diiodo-1,4-butadiene (10 examples) or dibromo analog (three examples). Conversion to the dilithio-1,4-butadiene and quenching with $Si(OMe)_4$ provided the silole 2,5-R_2-3,4-$R'_2C_4Si(OMe)_2$ (21–52%) [58].

1.3.4.1.2 Exchange of Zr in Zirconacycles for Si The formation of main group heterocycles from zirconacyclopentadienes was reported by Fagan and Nugent in 1988 and is referred to as the Fagan method. The approach was not successful with the reaction of $Me_4C_4ZrCp_2$ and $SiCl_4$ [59a] but was subsequently shown to be fairly successful in the preparation of $Me_4C_4SiBr_2$ using $SiBr_4$ [59b]. Later, Kanno and Kira demonstrated room-temperature exchange reactions from chlorosilanes and also the isolation of several siloles (88–97% yield) from $Me_4C_4ZrCp_2$ ($MeHSiCl_2$, $PhMeSiCl_2$, SiF_4), $Et_4C_4ZrCp_2$ (H_2SiCl_2), and $(Me_3Si)_2Me_2C_4ZrCp_2$ (H_2SiCl_2). The reaction exhibited a solvent dependence with the rate decreasing in the order CH_2Cl_2, $CHCl_3 > C_6H_6 \gg$ THF. The exchange reactions are 'critically affected by steric factors of the zirconacycles and the halosilanes' [59c].

These two basic reactions (iodination and exchange) are summarized in Equation 1.5.

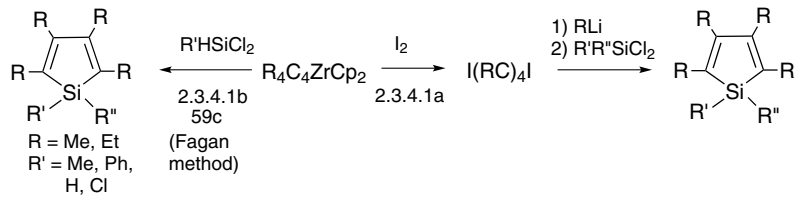

(1.5)

1.3.4.2 Siloles from Metal-Catalyzed Reactions

The first transition metal-catalyzed formation of siloles was reported by Kumada and co-workers in 1972, from the reaction of $HMe_2SiSiMe_2H$ and $RC{\equiv}CR'$ ($R = R' = Ph$, Et; $R = Ph$, $R' = Me$; $R = Bu$, $R' = Me$) catalyzed by $NiCl_2(PEt_3)_2$ (<1 mol%) in yields ranging from 44 to 100%, with the highest yields from the reaction of alkyl-substituted alkynes [60a]. The unsymmetrical alkyne with $R = Ph$, $R' = Me$ gave one regioisomer but that with $R = Bu$, $R' = Me$ gave three isomeric siloles. No other disilane could be used successfully, hence the method is restricted to siloles with only exocyclic Me substituents at Si. Since then, other publications have appeared utilizing $NiCl_2(PEt_3)_2/HMe_2SiSiMe_2H$ for the formation of two sets of siloles with dendrimer substituents. The reaction of 1,2-bis(3,5-dihydroxyphenyl)acetylene with benzyl ether-type dendritic bromides provided the alkyne precursors through the third generation and provided siloles of the type $R_4C_4SiMe_2$ with dendrimer substituents on all ring carbon centers [60b,c]. Fluorescence spectra were recorded in solution with attendant Φ_{PL} values. The same group reported another set of siloles with dendrimer units in only the 2,5-position from reaction of a tethered diyne with the same catalyst system [60d]. In this case, quantum yields for solution spectra were provided and, although films were cast from toluene, Φ_{PL} values were not reported. A related catalyst system, $Ni(acac)_2/PEt_3$/DIBAH, has been used to prepare a 2,5-bis(2-thienyl)silole (DMTS) from a 2-thienyl-terminated, tethered diyne [60e]. The quantum yield was reported only for the solution of the silole. More recently, a Rh-catalyzed reaction of internal alkynes and dialkynes with $Me_3SiSiMe_3$ has been introduced as a route to siloles. The best conditions for the reaction involve the use of $[RhCl(nbd)]_2$ (5 mol%) in THF at 50 °C in the presence of 30 mol% of nbd (norbornadiene). DMTS was formed in 76% yield from PhC≡CPh [60f]. There are certain difficulties with this method, including workup, which requires preparative TLC. It should be noted that these two transition metal-catalyzed routes to DMTS (summarized in Equation 1.6) provide a more straightforward route to this silole, the blue emission of which was described in 2001 by Tang *et al.* [16] and previously prepared by the Curtis method. The use of aliphatic alkynes (e.g. 4-octyne) was unsuccessful. With unsymmetrical alkynes, an inseparable mixture of products with three possible isomers was formed. Tethered 1,6-diynes gave moderate yields of siloles [60f]. The reaction of no other starting disilane was reported.

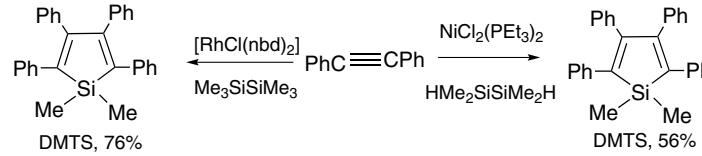

(1.6)

There are $(Ph_3P)_2PdCl_2$-catalyzed reactions of alkynes with silacyclopropanes or silacyclopropenes, but this would not be a practical synthesis for siloles. However, other transition metal-catalyzed reactions have

been reported that produce different substitution patterns of the silole core. An interesting Pd-catalyzed reaction with $Pd(dba)_2/PPh_3$ (or other bulky phosphines) of terminal alkynes with an $(Et_2N)Me_2Si—B(pin)$ showed high regioselectivities ($\geq$90:10) for the 2,4-substituted silole. The isolated yields from PhC≡CH or $XC_6H_4C{\equiv}CH$ were 78–96%. The 5-position of 1,1-dimethyl-2,4-diphenylsilole could be brominated and the bromide was used for cross-coupling with $Bu_3SnC{\equiv}CAr$ [61a]. A related study by Suginome with the same silylborane and substituted butadienes utilized $Pd(dba)_2/PMePh_2$ to generate variously substituted silacyclo-3-pentenes and a few examples were then reacted in a separate step with *p*-chloranil [or DDQ (2,3-dichloro-5,6-dicyanobenzoquinone)] to give a silacyclopentadiene [61b]. Both of these methods give a unique, partially substituted silole core.

Although not commonly used, dihydrosilanes can provide siloles through hydrosilylation reactions. 1,3-Diynes undergo a double hydrosilylation to give 2,5-diarylsiloles and the reaction is promoted by the precatalyst $[Cp^*Ru(MeCN)_3]PF_6$ [62a]. The reaction of 1,4-diphenyl-1,3-butadiyne with Ph_2SiH_2 provided ~50% yields of 1,1,2,5-tetraphenylsilole but gave virtually no silole product when Et_2SiH_2 or $PhMeSiH_2$ was utilized. Specific formation of the same 1,1,2,5-tetraphenylsilole was reported previously from the Tamao procedure that started with phenylacetylene and $Ti(O^iPr)_4/{}^iPrMgCl$ to provide the 1,4-diiodo-1,4-butadiene that was lithiated and converted to the silole (21% yield) through reaction with $Si(OMe)_4$ [58]. Another route to 1,1-dimethyl-2,5-diarylsiloles involved the reaction of 1,3-diynes first with Li_2Te to give the tellurophene, which could be ring opened with ^{t}BuLi and treated with Me_2SiCl_2 to give the silole (Ar = Ph, 59%; four other examples) [62b]. It is likely, however, that siloles without 3,4-substituents (β to the Si) will exhibit the AIE property. More complex silole systems were also prepared by the double hydrosilylation of 1,3-dialkynes [62a].

1.4 Modification of Preformed Siloles

In the previous section, the various methods of forming siloles were outlined. In some of these methods, the synthesis provided functional groups at either silicon or carbon. The role of these substituents in forming new siloles is the focus of this section.

1.4.1 Reactions at silicon centers

The basic functional groups at silicon include Si—Cl, Si—H and Si—OMe and are outlined generally in Scheme 1.1.

Exocyclic Si—Cl bonds of siloles are formed *in situ* in the Curtis method (Section 1.3.1) when either $SiCl_4$ or $RSiCl_3$ is used to quench the dilithiobutadiene formed from tolan. The substitution of these Si—Cl bonds with active organometallic reagents (e.g. R′Li and R′MgX) will produce siloles with exocyclic

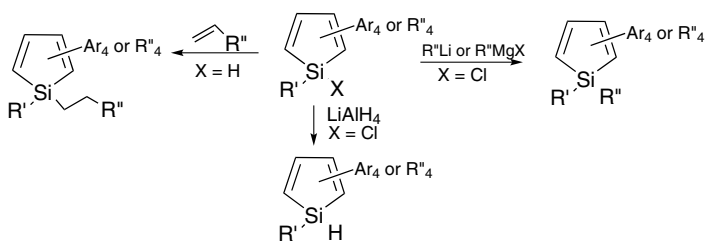

Scheme 1.1 *General substitution reactions at silicon centers.*

organic groups. Any Si—Br, Si—F or Si—OMe bonds will react similarly although a promoter (CuCN) is required in the last case. Another useful reaction of Si—Hal bonds is reduction with $LiAlH_4$ to Si—H bonds. Hydrosilanes add across multiple bonds, which is a principal method for Si—C bond formation. As an example, Ph_4C_4SiMeH reacts with allylamine (H_2PtCl_6 precatalyst) to form $Ph_4C_4Si(Me)CH_2CH_2CH_2NH_2$. Although not described as AIE, the silolepropylamine was converted to nanoparticles by addition of water to a THF solution, which produced significantly enhanced fluorescence (up to 46 times that of a THF solution). The nanoparticles were a selective chemosensor for CrO_4^{2-} in the presence of other oxyanions [63a]. The silolepropylamine, when treated with MeI, produced $Ph_4C_4Si(Me)CH_2CH_2CH_2NMe_3^+I^-$ where the AIE effect was also utilized for DNA sensing [63b], and has been used similarly for other biomolecules (for additional examples see Section IVA in [8c]).

1.4.2 Reactions of a ring carbon center

The majority of the reactions at 2,5-carbon centers of siloles involve 2,5-dihalosilole precursors. The 2,5-dihalosiloles can be formed directly from the Tamao procedure (Section 1.3.2). A more indirect route through a 2,5-bis(trimethylsilyl)silole has been developed using $PyHBr_3$ to cleave the $Me_3Si—C_{core}$ bond [64a]. The method exhibits some problems as the brominating reagents can also attack the $Si—C_{ring}$ bond. This side reaction can be suppressed by utilizing relatively 'bulky' exocyclic substituents at silicon, particularly 1,1-(^{i}Pr)$_2$siloles at low temperature, but the yields are still modest. An alternative route involves generating the zirconacycle from $Me_3SiC{\equiv}CMe$ and $Cp_2ZrCl_2/^n$BuLi *in situ* followed by treatment with I_2 [64b] or through a comparable titanacycle [58] and cleavage with $PyHBr_3$, I_2 or ICl. The use of $ICl/AgBF_4$ gave useful yields even when 1,1-substituents were Me or Et. Reaction of the dihalosilole with 1 equiv. of ^{n}BuLi at −78 °C and quenching with either ^{n}Bu$_3$SnCl or a 2-^{i}PrO-1,3,2-dioxaborolane provided incorporation of one substituent that could be used with different cross-coupling conditions [64a]. Several examples of cross-coupling reactions to provide substituted siloles can be found in Table 11 in [8c].

1.5 Related Germole Methodology

The synthetic procedures providing germoles are very undeveloped relative to those outlined for siloles. There are only two commonly used protocols and both of these involve alkyne precursors and mimic the dilithiobutadiene salt metathesis approach (Curtis procedure, Section 1.3.1) and the zirconacycle exchange approach (Fagan procedure, Section 1.3.4.1) illustrated for siloles. Most importantly, the Tamao approach used so effectively for siloles fails. Consequently, the germoles that have been isolated generally bear the same substituents at all the carbon centers of the germole core in the two commonly used methods. There are two other methods that may hold some promise for future development and these are described briefly in Section 1.5.2. The reactions described closely parallel those in silole chemistry.

1.5.1 Germoles produced by metathesis and exchange reactions

The dimerization of PhC≡CPh with Li to produce LiPhC=CPh—CPh=CPhLi and subsequent treatment with germanium chlorides (and other main group halides) was first described by Leavitt *et al.* in a communication [65a] and subsequently with experimental detail in a full paper [65b]. Although $Ph_4C_4GeCl_2$ appears to be reported, it is the spirocycle $Ph_4C_4GeC_4Ph_4$ that was actually described. In the full paper, the intermediate $Ph_4C_4GeCl_2$ could not be identified and attempts to prepare other related germanium derivatives were unsuccessful, with elemental analyses that could not be reproduced. Several years later, Hota and

Willis reacted 1,4-$Li_2Ph_4C_4$ with Me_2GeCl_2 in diethyl ether and after removal of the ether and extraction with CH_2Cl_2 obtained $Ph_4C_4GeMe_2$ in satisfactory purity [65c]. However, when the method employed by Levitt *et al*. of precipitating the product from CH_2Cl_2 with MeOH, was used by Hota and Willis, only tetraphenylbutadiene was obtained. Curtis reported the first successful isolation of $Ph_4C_4GeCl_2$ in 70% yield by reverse addition of 1,4-$Li_2Ph_4C_4$, prepared in diethyl ether, to $GeCl_4$ (the spirocyclic by-product was additionally isolated in 5% yield) [65d]. $Ph_4C_4GeCl_2$ has also been reported with somewhat different conditions in yields of 80% [65e] and 27% [65f]. Curtis also reported the preparation of an additional germole, $Ph_4C_4GePhCl$ (47%), from $PhGeCl_3$ [65g]. The germoles $Ph_4C_4GeH_2$ and Ph_4C_4GePhH were prepared from the respective chlorides and $LiAlH_4$ [65h]; however, the experimental details were provided only in the supplemental material.

It is the chlorogermole or the hydridogermole that is useful for further manipulations. The reaction of $Ph_4C_4GeCl_2$ with 2 equiv. of RMgX provided $Ph_4C_4GeR_2$ (R = Et or aryl) and with 1 equiv. provided Ph_4C_4GeRCl (R = aryl), which, in turn, was reduced with $LiAlH_4$ to give the corresponding Ph_4C_4GeRH [65h]. The GeCl bond in $Ph_4C_4GePhCl$ reacted with 2 equiv. of Li to give an anion, which, when quenched with Me_3SiCl, gave $Ph_4C_4Ge(SiMe_3)Ph$ [65h]. A related approach has also been used with $Ph_4C_4GeCl_2$ but with a mixture of Mg and R_3ECl in THF to give $Ph_4C_4(ER_3)_2$ [R = Me, E = Si (87%); R = Et, E = Ge (85%)] [65i]. Reaction of $Ph_4C_4GeCl_2$ with 2 equiv. of LiC≡CR gave $Ph_4C_4Ge(C{\equiv}CR)_2$ {R = H, ^{t}Bu, Ph [65j]; R = Ar (seven examples), 3-thiophene, 2- and 3-pyridinyl, $P(Ph)_2$ [65k]}. Hence the substitution reactions of Ge—Cl in the germoles are very similar to those reported in the corresponding silole chemistry (summarized in Scheme 1.1).

The second major method for generating germoles involved the transmetallation of $Cp_2ZrC_4R_4$ (R = Me, Ph), which was first reported by Fagan and co-workers [66a,b]. The germole $Cl_2GeC_4Me_4$ was prepared from $Cp_2ZrC_4Me_4$ and $GeCl_4$ in THF at room temperature in 83% yield [66b]. The exchange method was studied more systematically by Dufour and co-workers [66c], who reported the reaction of various germanium halide precursors with $Cp_2MC_4Ph_4$ (M = Ti, Zr) and $Cp_2MC_4Me_4$ (M = Zr, Hf). Yields for the formation of $Ph_4C_4GeCl_2$ from $Cp_2MC_4Ph_4$ with $GeCl_4$ at room temperature in THF were 90% (M = Ti) and 80% (M = Zr). The authors also reported exchange of Me_2GeCl_2 with $Me_4C_4ZrCp_2$ and with $Me_4C_4HfCp_2$ (80 °C) to give the germole in 60% and 45% yields, respectively. Other germanium halides that were studied included $MeGeCl_3$ and $PhGeCl_3$ but the germole from the former was unstable and from the latter was isolated in low yield after reaction with $LiAlH_4$. The bulkier Ph_2GeCl_2 gave only a trace of germole product. Also, $Cp_2MC_4Me_4$ (M = Zr, Hf) was reacted with $GeBr_4$ but the yields were the same as with $GeCl_4$, hence there is no inherent advantage to using the bromide, at least in this case. In a subsequent study, the authors reacted $Me_4C_4GeCl_2$ with PhMgBr in diethyl ether (−70 °C) followed by $LiAlH_4$ and obtained Me_4C_4GePhH in 80% yield [66d]. Meier-Brocks and Weiss also prepared $Ph_4C_4GeCl_2$ and $Ph_4C_4GeMe_2$ by exchange of the zirconacycle with $GeCl_4$ and Me_2GeCl_2 in 45 and 95% yield, respectively [65j]. Tamao and co-workers used the exchange route in a one-pot process to obtain 1,1-diethyl-3,4-trimethylene-2,5-di(2-thienyl)germole starting from 1,7-dithienyl-1,6-heptadiyne, Cp_2ZrCl_2 and ^{n}BuLi followed by removal and exchange of the Et_2O solvent for toluene before Et_2GeCl_2 was added. A 2,5-di(2-thienyl)germole was isolated in 23% yield [60e]. Nitschke and Tilley developed a more complex target using the zirconocene exchange route with $GeCl_4$ to provide macrocycles with triangular geometries and 1–3 benzene linkers on the sides in 89–93% yield [66e].

1.5.2 Germoles from other methods

The synthetic aspects of germole chemistry do not appear to have been comprehensively reviewed since 1990, when Group 14 metallole chemistry was summarized by Dubac *et al*., and briefly by Armitage in 1996 [8a]. Only the most general methods will be outlined in this section.

There are two methods of approach to the formation of germoles that merit mention. In the 1980s, Wrackmeyer's group produced siloles and germoles from dialkynylsilanes and -germanes with BR_3 (see Equation 1.4) [67a]. In this particular ring-closure reaction, rearrangement occurs and the terminal group on the acetylene becomes the substituent in the 2,5-positions. In one of the earlier papers, germoles from reaction of $Me_2Ge(C{\equiv}CSnMe_3)_2 + BR_3$ provided two examples of germoles with $SnMe_3$ substituents in the 2,5-positions and $-BR_2$ and –R in the 3,4 positions, as deep-yellow oils that were claimed to be pure after removal of the volatiles (analyses were off). The materials decomposed on distillation at 100 °C/10^{-2} Torr [67a]. Formation of germoles from $Me_2Ge(C{\equiv}CMe)_2$ or $^{n}Bu_2Ge(C{\equiv}CMe)_2$ was briefly mentioned in [51], but the work was unpublished. Two 1,1′-spirobigermoles were reported from $Ge(C{\equiv}CR)_4$ and Et_3B [R = Me (84.5%), Ph (44%)], both of which were stable, and the latter was isolated as a solid. In both cases, the $-BEt_2$ group was removed with $MeCO_2H$ to give a distillable product when R = Me and a solid when R = Ph [67b]. An interesting variation was also reported using the precursor $Me_2Ge(C{\equiv}COMe)_2$ and Et_3B to give the 2,5-dimethoxygermole [67c].

Another promising approach to 2,5-disubstituted germoles from dialkynes was developed by Murakami and co-workers, involving a Ru-catalyzed *trans*-hydrogermylation [67d]. When 1,4-diphenyl-1,3-butadiyne and Ph_2GeH_2 were reacted in the presence of 10 mol% of $[Cp^*Ru(MeCN)_3]PF_6$, a 93% yield of the 1,1,2,5-tetraphenylgermole was obtained (Equation 1.7). Ten other symmetrically substituted 1,3-diynes also were studied and gave germoles in yields ranging from 70 to 93%. Three Ar—C≡C—C≡C—Ar′ and one Ar—C≡C—C≡C—R were also reacted with Ph_2GeH_2 and gave germoles with two different substituents in the 2,5-positions. The UV–vis spectrum of $Ph_2GeC_4Ph_2H_2$ exhibited a maximum absorption that was shorter than that of the corresponding silole but the germole had a higher fluorescence quantum efficiency in hexane (0.81) than the silole (0.64) [67d]. One example of the addition of Bu_2GeH_2 to Ph—C≡C—C≡C—Ph was also reported to give the germole (56% yield). Extension of the method to the phenyl-terminated tetrayne gave a novel 2,2′-bigermole [67d].

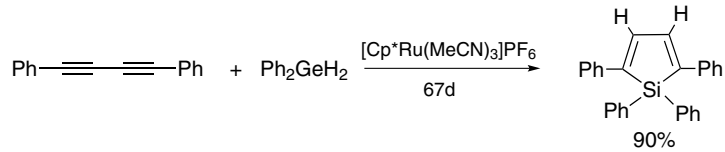

(1.7)

There are other minor methods, including the reaction of dimethylgermylene, which adds to alkynes in the presence of catalytic amounts of $Pd(PPh_3)_4$ to give regioselectively the 2,4-disubstituted germole from 1-hexyne, ArC≡CH (Ar = *o*-tolyl), and RC≡CR′ (R = CO_2Me, R′ = Me; R = CO_2Et, R′ = Ph). The products are all characterized by boiling point and spectroscopically, but only in the case of the germole from 1-hexyne was a yield specified (>90%). However, to access these germole systems required the generation of Me_2Ge from 2,3-benzo-7,7-dimethyl-7-germanorbornadiene, which, in turn, is formed from $Ph_4C_4GeMe_2$ and a benzyne intermediate [67e].

The number of successful synthetic routes to germoles at present is seriously limited. There is no flexible route to substituted germoles where the 2,5-substituents can be manipulated as is the case with the Tamao procedure for siloles. It is the substitutents in these positions that appear to affect most the electronic properties of the silole and therefore this could also be expected to be the case for the germole. Unfortunately, the Tamao procedure fails to provide germoles. Although the double *trans*-hydrogermylation of 1,4-butadienes is certainly effective, the products contain no rotor-type substituents in the 3,4-positions and such substituents may be important to produce the AIE effect in these germoles. No attempt appears to have been made by Murakami and co-workers to observe fluorescence in a mixed water–solvent solution, therefore the possibility of the AIE effect in the germoles produced has not been determined [67d].

The reason behind the lack of germole formation upon the treatment of $R_2Ge(C{\equiv}CAr)_2$ with LiNaph has not been pursued. However, the Wrackmeyer method that does not involve a reductive C—C coupling gives germoles with substituents at each carbon center, although these may not be optimal to demonstrate any AIE effect. In principle, the exchange route could provide more flexibility in terms of substitution pattern, but that will depend on the metallocene that can be prepared from alkynes. The use of Ar—C≡C—Ar′ will give zirconocene isomers that then must be separated, adding additional complexity to the overall synthesis of the germole.

1.5.3 Photoluminescence and AIE of germoles

There are not many reported studies that include experiments that might reveal potential AIE effects in germoles and even fewer where the same systems for Ge and Si are compared. It is this comparison that allows the determination of the practicality of using one heteroatom over the other. Two studies by Mullin and co-workers reported comparisons of $Ph_4C_4MMe_2$ and $Ph_4C_4MPh_2$ (M = Si, Ge, Sn) for PL characteristics and the AIE effect [20, 68]. Optical characteristics were studied in various solvents, in rigid room-temperature glasses, solid pellets and in frozen dioxane solutions (−20 and −196 °C). The germoles are stronger emitters (higher quantum yields, Φ_F) than the siloles in the six solvents reported for the MMe_2 and MPh_2 systems; however, the siloles are better emitters in the solution aggregates (dioxane–water system) and also in the SOA glass (∼1.5–3.7 times greater in the SOA glass than in the aggregates in solution). Luminescence quantum yields of the aggregates were as high as 300 times greater than the values in dilute solution and exhibited no significant changes in the λ_{max} for the emission. The emission intensities of solutions increased on cooling by factors of 5–88 at −20 °C and by 31–134 at −196 °C. The enhancement of the PL on cooling is consistent with restricted rotational, vibrational and collisional degrees of freedom in the siloles and germoles studied. Mullin and co-workers also obtained the crystal structures of $Ph_4C_4MPh_2$ (M = Si [20], Ge [20], Sn [17]) and in each case there are two molecules in the unit cell. The closest contacts are CH contacts and these are to molecules in adjacent unit cells and none to the molecule in the same unit cell. The propeller nature of the metalloles apparently prevents a close approach and self-quenching does not occur. The ^{1}H NMR spectra of these six metalloles indicate a C_{2v} symmetry in solvents in which they are soluble, although the phenyl rings in the solid state are twisted out of the plane of the core with different dihedral angles. The equivalence of the 2,5-phenyl protons and of the 3,4-phenyl protons in the NMR spectra would be observed if the substituent phenyl rings rotate about the bond to the core carbon. Tracy *et al.* had reported calculations at the AM1 semiempirical level of theory for $Ph_4C_4MMe_2$ and $Ph_4C_4MPh_2$ [17], and a DFT calculation with the Gaussian 98 suite for $Ph_4C_4GeH_2$ (DHG) and $Ph_4C_4GeMe_2$ (DMG) was reported more recently by Kim and co-workers [69a] (without referring to the Tracy publication) and also summarized again in a report where the germoles were incorporated into OLED (organic light-emitting diode) devices [69b]. The numbering system used by Kim and co-workers is non-standard and thus confusing, hence the carbon positions of the ring will be identified here as α- and β- to the Ge center. The charge on the β-carbon is more positive than the charge on the α-carbon (consistent with the ^{13}C NMR resonance assignments with the β-C downfield of the α-C) [17] and the DFT calculations indicate that both the HOMO and LUMO are mainly localized in the germole ring and the two phenyl groups at the α-C [69a]. The calculated energy differences between the HOMO and LUMO were 3.699 and 3.821 eV for DHG and DMG, respectively [69b]. More recently, Kim and co-workers prepared OLEDs with $Ph_4C_4Ge(C{\equiv}CPh)_2$ (HPAG) as host material and 4-(cyanomethylene)-2-methyl-6-(*p*-dimethylaminostyryl)-4*H*-pyran (DCM1) as a guest molecule (together as the emission layer) and *N*,*N*′-diphenyl-*N*,*N*′-bis(3-methylphenyl)-1,1′-biphenyl-4,4′-diamine (TPD) as the hole transport layer. Host–guest Förster energy

transfers between HPAG and DCM1 provided a strong red-emission OLED. Such an OLED should be useful for red organic light-emitting device applications [69c].

Another recent publication reported AIE in 11 derivatives of $Ph_4C_4Ge(C{\equiv}CR)_2$, where R = 4-C_6H_4X (X = CF_3, OCF_3, Me, OMe, Ph, OPh), 3-C_6H_4F, thiophen-3-yl, 3-pyridinyl, 2-pyridinyl and –PPh_2, with crystal structures for nine of the examples [70]. The Φ_F values in CH_2Cl_2 ranged from 0.00457 to 0.00706 and Stokes shifts ranged from 117 to 132. The AIE effect was demonstrated in acetone–water systems, and for the 4-$C_6H_4CF_3$ case Φ_F was 65 times higher than that observed in acetone. The germoles were about three times more emissive in solution than siloles and thus exhibited a smaller enhancement of luminescence when aggregated. The AIE effect of the germoles for sensing VOCs (volatile organic compounds) was also demonstrated [70].

1.6 Metallaindenes and Metallafluorenes of Si and Ge

Aromatic annulated metalloles contain one or two rings fused to the metallole core. In most cases, these have been benzene rings (benzene-annulated systems), but more recently other heteroarenes such as pyridine fused to the metallole core have been reported and, in particular, in the case of fused thiophene rings have provided materials that have shown promise for incorporation into electronic devices. The core structures and numbering used for silaindenes and silafluorenes as representative of the annulated metalloles are illustrated in Figure 1.1.

1.6.1 Methods for the formation of silaindenes and germaindenes

Only selected synthetic examples will be described and a more complete discussion of silaindenes can be found in [71a]. Just as tolan was used in the early syntheses of siloles, the same starting material was used for the generation of silaindenes, but the reaction required 2 equiv. of ^{n}BuLi per mole of tolan in a 1:1 diethyl ether–THF solvent mixture for ~22 h (Equation 1.8). With added THF and warming to reflux, the addition of Me_2SiCl_2 gave the 1,1-dimethylsilaindene in 70% yield and the spirocycles were formed from both $SiCl_4$ (22%) and $GeCl_4$ (28%) [71b,c].The corresponding colorless 1,1-diphenylsilaindene was similarly reported in 46% yield and was described as exhibiting strong blue fluorescence in the solid state under UV irradiation [71b]. In a somewhat related method, *o*-($HSiMe_2$)$C_6H_4C{\equiv}CPh$, when treated with Me_3SnLi (formed from Li granules and $ClSnMe_3$), provided 2-phenyl-3-trimethylstannylsilaindene in 90% yield when conducted on a 20 mmol scale (Figure 1.3a) [71d]. Trimethylstannyl groups are useful (after transmetallation with $ZnCl_2$) in Pd^0 cross-coupling reactions [71d,e]. The polybenzo[*b*]siloles reported were incorporated as hole-blocking materials for phosphorescent OLEDs, the performance of which surpasses that of the standard that was current in 2010 [bathocuproine (BCP)] [71e].

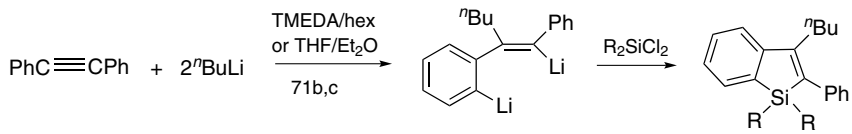

(1.8)

Formation of silaindenes using stoichiometric amounts of a zirconacycle precursor have been described. In one of these, the zirconacycle was reacted with iodine to provide 1-iodo-2-[(1*Z*)-2-iodo-1-methyl-1-propen-1-yl]benzene that was the starting point for the silaindene. The diiodobutadiene derivative was

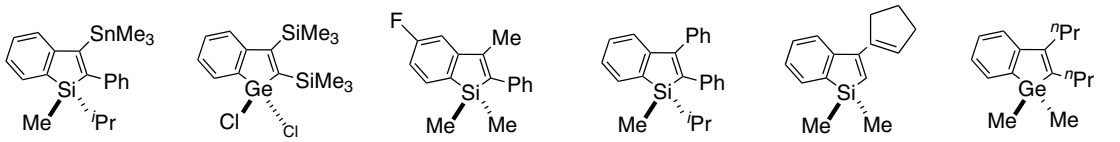

(a) 90% [71d] (b) 94% [71f] (c) 95% [71h] (d) 45% [71i] (e) 50% [71j] (f) 93% [71n]

Figure 1.3 *Variously substituted sila- and germaindenes.*

dilithiated with 2 equiv. of ^{n}BuLi in diethyl ether and subsequent reaction of the dilithio reagent with Me_2SiCl_2 provided the silaindene in 98% yield, and with 0.5 equiv. of $SiCl_4$ the related spirocycle was formed in 84% yield [55f]. Although silicon halides do not effectively undergo transmetallation with zirconacycles, $GeCl_4$ does. 1-Zirconaindenes are readily prepared from $Cp_2Zr(Me)Ph$ and RC≡CR′ in refluxing benzene [six examples, but the yield was provided only for the zirconacycle from $(Me_3Si)C{\equiv}CNEt_2$, 61%]. Reaction of the zirconacycles with $GeCl_4$ in THF at room temperature provided six 1-germaindenes (yields from 85 to 96%; example, Figure 1.3b) [71f]. With Cp_2ZrPh_2 and PhC≡CPh in refluxing toluene, 2,3-diphenyl-1-zirconaindene (71% yield) was produced, which formed 1,1-dichloro-2,3-diphenylgermaindene upon treatment with $GeCl_4$ (86% yield) [71g].

The more interesting recent transition metal-mediated routes to silaindenes involve a hydrosilane where ring closure utilizes an alkyne or an alkyne substituent on an arylsilane, and are only briefly described here and are summarized for the same target in Equation 1.9. The reaction of *o*-$Me_3SiC_6H_4Li$ (50% excess) with RC≡CR′ at 30 °C for R = R′ = Pr (the additional four examples at −20 °C) in the presence of $Fe(acac)_3$ (5 mol%) provided the benzosiloles in yields that were ∼92% for the symmetrical alkynes (R = R′, two examples) and from 73 to 91% for R ≠ R′ (three examples, R′ = Ph, 1-hexynyl), with R′ in the 2-position, although in this case minor amounts (≤6%) of a second isomer with R′ in the 3-position were observed (example, Figure 1.3c). Other examples reported included those with two or three benzosilole units connected to a benzene ring [71h]. In a related reaction, *o*-$Me_2{}^{i}PrSiC_6H_4Br$ and PhC≡CPh in refluxing toluene with $[PdCl(\pi\text{-allyl})]_2$, P^tBu_3, LiO^tBu, and 4-$O_2NC_6H_4CHO$ provided the 2,3-diphenylsilaindene in 45% yield (Figure 1.3d) [71i]. Several other silaindenes were formed from ArC≡CAr and ArC≡CSiR_3 in good yields. The results with aliphatic alkynes were less promising and another catalyst system was employed, consisting of $[Pd(PPh_3)_4]$ and K_2CO_3, and comparable yields were then obtained [71i]. A gold (I)–phosphine complex (^{t}BuXPhos) has been used to ring close *o*-$RMe_2SiC_6H_4C{\equiv}CH$ (R = *c*-C_5H_7), where *trans*-alkenylsilylation occurred to give 3-cylopentenyl-1,1-dimethyl-1-silaindene (50% yield) (Figure 1.3e) [71j].

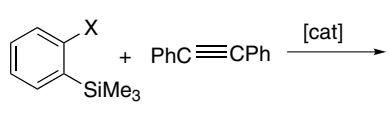

X	Catalyst	Yd
Li	$Fe(acac)_3$	93%
Br	$[PdCl(\pi\text{–allyl})$	90%
$B(OH)_2$	$[RhCl(cod)]_2$ + DABCO	97%

(1.9)

Aryl(2-ethynylphenyl)silanes undergo exclusive 1,1-arylsilylation (the same gold catalyst, refluxing CH_2Cl_2) to give 2-aryl-1-silaindenes (four examples, yields ranging from 24 to 64%) [71j]. Similar strategies have been reported using styrene derivatives although these are at least two-pot procedures. Lithiation of 2-bromostyrene and quenching with Me_2SiHCl provided the (2-vinylphenyl)silane, which was then reacted with terminal acetylenes {20 mol% $[Cp^*Ru(MeCN)_3]PF_6$} to give the *trans*-hydrosilylation product

of the alkyne (isolated) followed by ring-closing metathesis (RCM) with Grubbs II catalyst to give the 2-substituted-1-silaindene (eight examples with overall yields varying from 5.5 to 68%) [71k]. A one-pot procedure was utilized for conversion of aryl-substituted styrenes through hydrosilylation with H_2SiPh_2 $[NiBr_2(PPh_3)_2]$ followed by a dehydrocyclization reaction $\{[Ir(OMe)(cod)_2]_2$/dtbpy/norbornene$\}$ to give various aryl-substituted dihydrosilaindenes (18 examples, 49–86% yields) [71l]. The hydrosilylation–dehydrocyclization route was also utilized for α-substituted styrenes although the hydrosilylation was conducted in the presence of $B(C_6F_5)_3$ with yields of 79% (3-methyl-1-silaindene) and 76% (for the 3-phenyl derivative). The authors also demonstrated the dehydrogenation of the dihydrosilaindenes to the silaindene with DDQ (three cases, 73–81%) yields [71l].

The *trans*-hydrogermylation of *o*-$HMe_2GeC_6H_4C{\equiv}CPh$ with $[Cp^*Ru(MeCN)_3]PF_6$ (10 mol%) successfully produced the 2-phenylgermaindene although the yields were a modest 45% [71m]. Another route that involved $C(sp^3)$—Ge bond activation for a 2-trimethylgermylphenylboronic ester with $RC{\equiv}CR'$ catalyzed with $[RhCl(cod)]_2$ (5 mol%) and 2 equiv. of DABCO, gave high yields of 2,3-substituted-1-germaindenes [$R = R'$, eight examples, 65–93% yields (Figure 1.3f); $R \neq R'$, six examples, 44–91% yields]. When the alkyne had a phenyl substituent and an alkyl group, the phenyl group was incorporated at the position α to the Ge center [71n]. Two of the germaindenes, 2,3-diphenyl-1,1-dimethylgermaindene and the 2,3-*p*-$CF_3C_6H_4$ analog, were described as exhibiting intense PL in the solid state [71n].

In summary, as with siloles and germoles, the basic metallaindene can be formed from tolan and RLi (2 equiv.) via the dilithio reagent produced, although the R group is then incorporated into the 3-position of the product metallaindene. The exchange reaction with a zirconacycle is effective for producing the germaindene but not the silaindene. However, it would be interesting to see if Kira's method (Section 1.4.2) using small chlorosilanes would be effective. The recent variety of transition metal-catalyzed reactions of suitably substituted arylsilanes has provided reasonable to very good yields of metallaindenes with different substituent patterns for the 2,3-positions and also incorporating substituents on the benzo portion, which is more difficult to accomplish with the other routes. No experiments that would lead to the observation of the AIE effect have been reported even in the most recent publications. However, there are some indications that the metallaindenes could be useful in electronic devices.

1.6.2 Methods for the formation of metallafluorenes

Only selected synthetic examples will be described and a more complete presentation of silafluorenes can be found in [71a]. The first silafluorene was reported by Gilman and Gorsich in 1955 from reaction of *o*,*o*′-dilithiobiphenyl formed from the dibromobiphenyl precursor and ^{n}BuLi at −78 °C, followed by quenching with Ph_2SiCl_2 to give 9,9-diphenylsilafluorene in low yield [72a]. This lithiation route (with variations) still remains a primary route to silafluorenes. However, the focus over the last 10 years or so has been on the development of *o*,*o*′-dibromobiphenyl systems with additional substituents on the biphenyl rings, although these tend to be 'symmetrically' substituted on the two rings. This conventional method for the synthesis of 9-silafluorenes does not lend itself to formation of silafluorenes with different substituents on the two benzo rings as the requisite *o*,*o*′-biaryl must be synthesized from two different aromatic rings such that the bromides reside in the correct position. However, West and co-workers succeeded in preparing the appropriate unsymmetrical precursor to 9,9-dichloro-2,4-diphenyl-9-silafluorenes from a monobromide generated from commercial 1,3,5-triphenylbenzene, which was dilithiated (Li—Br exchange and *o*-CH metallation) and quenched with $SiCl_4$ (experimental conditions not described) [72b]. An alternative approach is the recently reported route using transition metal catalysts described later in this section. The multi-substituted biphenyls are described in tabular form in [71a] in addition to the silafluorenes that are generated from them. Appropriate substitution reactions of the CH bonds in the metallafluorenes have not yet been developed so

that any desired substituents should be in place on the starting biphenyl prior to the ring closure reaction that provides the sila- or the germafluorene.

A common objective in the synthesis of silafluorenes is the incorporation of replaceable units in the 2,7-positions of the carbon core of the product. Such units are usually C—Br or C—SnR_3 for use in cross-coupling reactions, particularly for polymer/copolymer formation. If the bromide substituents are incorporated into the starting biphenyl, then the halogen used for formation of the silafluorene (or germafluorene) must be the 2,2′-diiodobiphenyl as this halogen reacts preferentially with RLi in the exchange reaction to form the dilithiobiphenyl required for ring closure. A common substitution pattern (simplest tetrahalobiphenyl) would be 4,4′-dibromo-2,2′-diiodobiphenyl. Additional substituents could be present, as is the case for the diiodobiphenyl produced from *o*-dianisidine (Equation 1.10) [72c]. Lithiation of 6,6′-diiodo-4,4′-dibromo-3,3′-dimethoxybiphenyl followed by quenching with R_2SiCl_2 produced the silafluorene with R = Me (93% yield) and R = Ph (68% yield). Sonogashira cross-coupling with HC≡CAr in the presence of $Pd(PPh_3)_4$/CuI/piperidine produced four examples of the replacement of the bromide substituents with alkynyl substituents [72d]. This substitution produced silafluorenes that exhibited intense blue–green emissions with quantum efficiencies ranging from 0.46 to 0.89 [72d]. A more common use of bromide substituents is cross-coupling of units in polymer/copolymer formation. One example from germafluorene chemistry involved 2,7-dibromo-1,1-dialkylgermafluorene, where the bromide was used in two different ways. Coupling of the dibromogermafluorene with $Ni(cod)_2$/cod/2,2′-bipy gave two examples of a homopolymer. Lithiation of the dibromogermafluorene followed by treatment with 2-isoproxy-4,4,5,5-tetramethyl-1,3,2-dioxaborolane provided two dioxaborolanyl-substituted germafluorenes (differing in the R substituent at the Ge center) that were then utilized in Suzuki cross-coupling polymerization with aromatic halides to produce four alternating copolymers [72e].

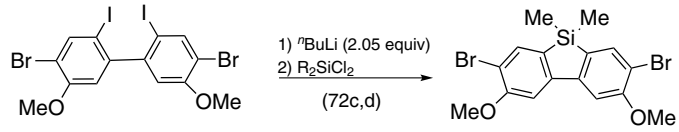

(1.10)

The more recent synthetic focus involves transition metal-promoted ring closure reactions. A variant that has been used to prepare both silafluorenes and germafluorenes from intramolecular arylation of a 2,2′-diiodobiaryl with a secondary silane or germane employed $Pd[P(^tBu)_3]_2$ as the catalyst in the presence of the base ($^iPr_2EtN$) (in the absence of base the reaction does not proceed) [72f]. The use of 2,2′-dibromobiaryls provided lower yields of the heterofluorene. Both Et_2MH_2 and Ph_2MH_2 (M = Si, Ge) were utilized but bulky silanes such as 1-NpPhSiH_2 or $(^tBu)_2SiH_2$ did not react, possibly owing to steric crowding. In addition to silafluorene (88–89% yield) and germafluorene (87–88% yield), three additional examples of symmetrically substituted biaryls produced 9,9-diethylsilafluorenes (yields from 64 to 81%), 9,9-diethylgermafluorenes (yields from 55 to 83%), 9,9-diphenyl-silafluorenes (yields from 40 to 62%; Figure 1.4a), and

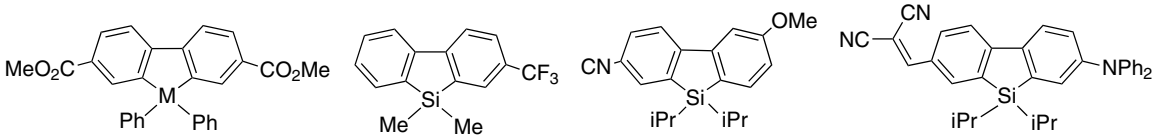

(a) M = Si, 40% [72f]
(b) M = Ge, 26% [72f]
(c) 95% [72g]
(d) 95% [73a]
(e) 48% (3 steps) [73b]

Figure 1.4 *Selected silafluorenes.*

9,9-diphenylgermafluorene (yields from 26 to 43%; Figure 1.4b) (Equation 1.11). The systems with electron-accepting substituents had higher Φ_F values than those with electron-neutral or electron-releasing substituents. One example exhibited a Φ_F value of 0.59 in the solid state ($\Phi_F = 0.32$ in CH_2Cl_2). The difference was attributed to $C{=}O\cdots H{-}C_{arom}$ and also a $C{=}O\cdots C{=}O$ interactions in the solid that produced a more compact J-type aggregation structure. It was the hydrogen bonds that provided the luminescent color change [72f].

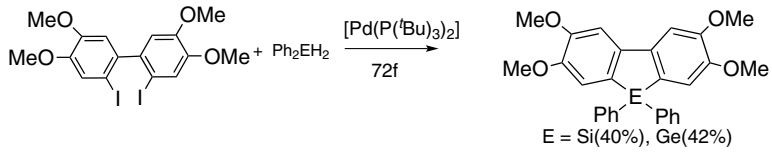

(1.11)

Another transition metal-catalyzed silafluorene synthesis involves activation of both an SiH and a CH bond of a biphenylhydrosilane utilizing Wilkinson's catalyst (0.50 mol%) in dioxane at 135 °C (Equation 1.12) [72g]. Other Rh catalysts such as $[RhCl(cod)]_2$, $[Rh(OAc)_2]_2$, $Rh_4(CO)_{12}$, and $RhCl(CO)(PPh_3)_2$ were less effective and other metal complexes containing Cr, Mo, W, Re, Fe, Co, Rh or Pt did not provide any silafluorene product. Biaryl groups that were substituted on one of the phenyl rings provided the silafluorene with a substituent on one of the rings. A substituent that is *para* to the ring junction of the biphenyl becomes a substituent in the 2-position of the silafluorene. If originally in the *meta* position, it becomes *para* to the Si center in the silafluorene. Isolated yields reported for 14 examples varied from 63 to 98% (an example is shown in Figure 1.4c). In one case, a yield of 69% was raised to 94% in the presence of a hydrogen acceptor ($CH_2{=}CHCH_2CMe_2H$). Construction of ladder molecules was also described (see also [71a]) [72g].

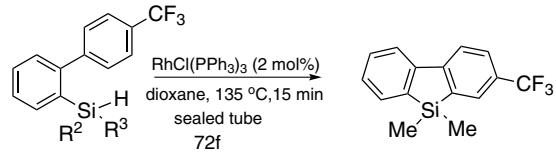

(1.12)

Siloles were prepared by Pagenkopf and co-workers using the Tamao procedure (Section 1.3.2) to incorporate electronically dissimilar functional groups at the 2- and 5-positions by sequentially incorporating an electron-poor acceptor alkyne and then the electron-rich donor next (one pot) [39]. Increasing the degree of electron delocalization in siloles from $Me_2SiC_4Ph_2(C{\equiv}CC_6H_4\text{-}A\text{-}p)(C{\equiv}CC_6H_4\text{-}D\text{-}p)$ relative to the parent (A = D = H) results in a stepwise bathochromic shift in the electronic absorption (from $\lambda_{max} = 429$ to 496 nm) and also the PL spectra where the longest wavelength emission was $\lambda_{max} = 649$ nm. How can this type of electronic manipulation be utilized in silafluorenes? An approach to this synthetic problem was introduced by Shimizu *et al.* in 2008 through the use of $Ar(Ar')SiR_2$ where one of the aryl groups contains an *o*-triflate substituent [73a]. Treatment of such silanes (no additional Ar or Ar′ substituents) in the presence of $Pd(OAc)_2$ (5 mol%), PCy_3 (10 mol%), and Et_2NH (2 equiv.) provided ring closure to give silafluorenes with different R groups (R = Et, ^{n}Bu, ^{n}Hex, ^{i}Pr, Ph) on silicon in yields ranging from 63 to 92%, except for the Et case where the yield was 39%. This first report also included a few examples of carbon ring substituents (Figure 1.4d). A later publication by Shimizu *et al.* provided additional silafluorenes where one of the benzo rings contained a substituent (four examples) and both rings contained a substituent (two examples) (yields from 88 to 98%; Figure 1.4e) that involved elaboration of the carbon substituent. The key to this method was the use of bulky substituents on silicon and the addition of the Et_2NH base [73a,b]. In a

more elaborate case, a tetracyclic product where one of the Si—Ar groups was a benzoindole was reported and exhibited high quantum yields not only in solution but also in the solid state (microcrystal, powder, thin film) and in poly(methyl methacrylate) (PMMA) where $\Phi_f = 1.00$ with intense blue emission [73a]. Therefore, the stage was set for the synthesis of 2-amino-7-acceptor-9-silafluorenes. Starting from variously substituted silanes, $ArSi(^iPr)_2Ar$ [Ar = 2-R-6-(OTf)C_6H_3–; R = H, CF_3, CN; and Ar′ = 2-(R_2N)C_6H_4–; R = Me, Ph], eight examples of 2-(NR^1_2)-7-R^2-9,9-diisopropylsilafluorene [R^1 = Me, R^2 = H, CF_3, CN, CHO; CH=C(CN)$_2$; R^1 = Ph, R^2 = CN, CHO, CH=C(CN)$_2$; the CH=C(CN)$_2$ requiring two additional steps] were prepared (one example, Equation 1.13) [73b].

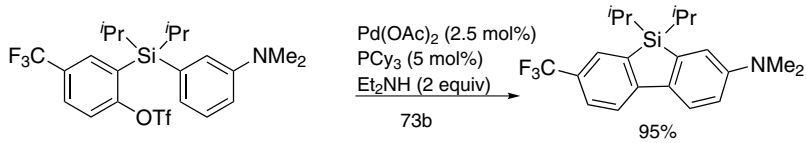

(1.13)

The fluorescence properties of all eight compounds in seven solvents were measured. The shortest λ_{max} for all the silafluorenes was observed in cyclohexane and the emission maxima were red- shifted with the electron-withdrawing nature of the acceptor. The difference between the shortest λ_{max} (c-C_6H_{12}) to the longest in DMSO varied for the 2-NR^1_2-substituted silafluorenes with R^1 = Me as 27 nm (R^2 = H), 49 nm (R^2 = CF_3), 63 nm (R^2 = CN), 127 nm (R^2 = CHO), and 205 nm [R^2 = CH=C(CN)$_2$]. Moderate to high Φ_f values were exhibited in solution by the silafluorenes with R^1 = Me, R^2 = CN, CHO, CH=C(CN)$_2$. A bathochromic shift in the neat thin film and in doped polymer films [polystyrene (PS), PMMA, polyacrylonitrile (PAN), and poly(ethylene glycol) (PEG)] was observed for the dimethylamino-substituted silafluorenes with quantum yields ranging from moderate to high. The Φ_f values for the diphenylamino derivatives were usually higher than those found for the dimethylamino derivatives in both neat and polymer films. DFT calculations indicated that the HOMOs of these D–π–A silafluorenes extended over the biphenyl and amino units. Although the LUMOs are delocalized on the acceptor, biphenyl and silicon bridges of the silafluorenes with A = H, CF_3, and CN, there is no lobe spread over the silicon bridges of the stronger acceptors [CHO, CH=C(CN)$_2$]. Thus, with a strong acceptor the silicon bridge does not participate in the delocalization of the π-system of the D–biphenyl–A skeleton [73b]. Shimizu and Hiyama published an account of the more recent developments of synthetic methods for silicon-bridged biaryls including silafluorenes [73c].

The successful synthesis of other silicon-bridged biaryls in fair to excellent yields has also been reported (six examples) [73d]. A unique application of the C—H bond functionalization used $Pd(OAc)_2$-catalyzed ring closure of a prochiral triflate ($Ar_2Ar'Si^tBu$) but in this case with various chiral ligands (Josiphos, MeDuphos, and QuinoxP*), to produce stereogenic dibenzosiloles [11 examples with enantiomeric excess (*ee*) generally >90%]. An interesting feature of this report is one of the very few examples where reaction of the carbon core of a silafluorene took place in reasonable yields to give a brominated product. 2-Methoxy-9-*tert*-butyl-9-phenylsilafluorene was brominated with NBS in MeCN to give a Br substituent *para* to the MeO group in 87% yield, and with *n*-BuLi–TMEDA (tetramethylethylenediamine) followed by $BrCF_2CF_2Br$, the bromine was introduced *ortho* to the MeO group in 64% yield [73d].

Metallofluorenes are still most commonly prepared by reaction of a suitable *o*,*o*′-dihalobiphenyl. In more recent cases where there are additional substituents on the carbon centers, the more difficult part of forming a metallofluorene is the synthesis of the substituted biphenyls. The synthetic techniques for introducing substituents on to a core carbon center in a metallofluorene have not yet been developed, at least in a general way. The advent of transition metal-catalyzed reactions of diarylsilane precursors has, however, led to metallofluorenes with additional carbon core substituents and also allows for building systems where the two

benzo rings are not identically substituted. This then can allow for electronic tuning, especially if the substituents are in the 2,7-positions. The disadvantage could be the necessity for 'building' the appropriate silane precursor with two different ArAr′ groups. It is still not common practice to test for the AIE effect, hence its presence or absence is generally not reported.

1.7 Oligomers and Polymers of Metalloles and Benzene-Annulated Metalloles

The most common oligomers (Section 1.7.1) and polymers (Section 1.7.2) are constructed from reactions either at the silicon (or germanium center) or from the carbon portion of the framework. A direct linkage of one metallole to another through the heteroatom produces both oligomers and polymers (polysiloles and polygermoles). However, the linking of metallole units with organic fragments can occur through either the heteroatom or the carbon framework. If linked through the carbon framework, this will generally be through the 2,5-positions of a metallole or the 2,7- or 3,6-positions of a metallofluorene. In general, this requires a halogen substituent or a –B(epin) (or related boron substituent) in the indicated positions as these are required for cross-coupling reactions in building polymeric systems for both homopolymers and heteropolymers. The oligomers are described in Section 1.7.1 and the higher molecular weight polymers in Section 1.7.2. Metalloles can also be attached to a polymer chain as pendant groups (Section 1.7.3) and have been formed in hyperbranched polymers (Section 1.7.3) The silaindene framework is found in ladder 'polymers' (Section 1.7.4). Polymers that contain silafluorene units are described in Section 1.7.5 and the related germanium oligomers and polymers in Section 1.7.6. Additional examples of all of the types of oligomers and polymers for the silicon systems may be found in [8c] and [71a].

1.7.1 Oligomers that contain silole units connected at the 1,1- and 2,5-positions

Although Si—Si bonds are often formed by Wurtz coupling of chlorosilanes, the reactions of R_2SiCl_2 are difficult to control. However, the condensation of $Ph_4C_4SiCl_2$ with 1.2 equiv. of Li, Na or K in THF at room temperature provided $Cl(Ph_4C_4)_nCl$ [$n = 3$ (47%), 4 (25%)] and $(Ph_4C_4Si)_x$, which were separated by preparative gel permeation chromatography (GPC) and X-ray structures were determined for the trimer and the tetramer.

When the reaction was conducted with 2 equiv. of metal in THF at reflux, followed by quenching with MeOH, the longer oligomer, $MeO(Ph_4C_4Si)_nOMe$ ($n \approx 15$, end-group analysis by ^{1}H NMR) was formed (37% from Li) [74a]. Another approach utilized $Ph_4C_4SiH_2$. The dehydrocoupling reaction was conducted with four catalyst systems: H_2PtCl_6, $Pd(PPh_3)_4$, $ClRh(PPh_3)_3$, and $ClRh(PPh_3)_3$/cyclohexene in toluene at reflux [74b]. With $ClRh(Ph_3)_3$, the dimer precipitated on cooling, but when the hydrogen acceptor, cyclohexene, was present the formation of the dimer was suppressed and longer oligomers were obtained. The M_w values were determined by GPC and M_n values by both IR and ^{1}H NMR spectroscopy for all catalytic runs reported. It was the opinion of the authors that the NMR integration method gave the most reliable results [74b]. The dimers $C_4Ph_4SiH—HSiPh_4C_4$ and $C_4Ph_4SiMe—MeSiPh_4C_4$ were more strongly luminescent than their respective monomers.

Trogler and co-workers also reported two different systems where three monomers were connected through the 1-position by vinyl groups [74c] and two monomers were connected by *p*-divinylbenzene units [74d]. Both sets included a silole 'trimer' (dimer [74c]) and a silafluorene 'trimer' (dimer [74c]) in addition to related polymers (presented in Section 1.7.2) that were utilized for the detection of nitroaromatic systems. The vinylene 'trimer' with silafluorene units exhibited a Φ_{rel} for thin films (relative to 9,10-diphenylanthracene) that was higher at 6.1% than that for the silole 'trimer' (0.4%) [74c]. Calculations for the trimers as models for the polymers were performed to obtain estimates of bandgap energies. LUMO

energies correlated with measured redox potentials of TNT, RDX, and HMX. The primary focus of the study with divinylbenzene spacers was the study of the properties of the polymer.

In a systematic study of silole oligomers that contained *p*-dialkynylbenzene spacers, Pagenkopf and co-workers demonstrated the synthetic strategies for the formation of oligomers with 2–5 silole units. The routes involved the use of asymmetric building blocks for end caps or designed to start the next reaction for chain extension. The routes demonstrate the power and flexibility of coupling reactions. In their experience, Sonagishira conditions gave erratic results and cross-coupling was achieved more reliably with Stille or Negishi conditions (performed with alkynylstannane or zinc acetylide, respectively) [74e]. From electronic absorption and PL measurements, the effective conjugation length in the corresponding silole polymers appears to be approximately equal to the tetramer (estimated from absorption maxima). The trimer through the pentamer exhibited extinction coefficients $>1.2 \times 10^5\,M^{-1}\,cm^{-1}$, suggesting that these oligomers might be good candidates for photovoltaic applications. The quantum efficiencies range from 9% for the monomer, 3% for the pentamer to ~0.3% for the other oligomers. The absorption maxima exhibited by the oligomers occurred at a longer wavelength than for the related oligo(aryleneethynylene)s [74e].

1.7.2 Polysiloles and silole polymers connected through 2,5-positions

Polysiloles are prepared by condensation of R_2SiCl_2 with an alkali metal (see Section 1.7.1). Condensation of $Ph_4C_4SiCl_2$ with Li provided a polysilole with $M_n = 5500$ [by size-exclusion chromatography (SEC)]. When a THF solution of the polysilole that was weakly luminescent was injected into water, nanoparticles were produced that were highly fluorescent and the intensity of the nanoaggregates increased ~17.8-fold when the solution contained 99% water, thus exhibiting the AIE effect. The intensity of 90% water solutions remained unchanged for 1 month, indicating that the nanoparticles did not change in aggregation degree or degrade [74f].

Polymetalloles, $MeO(Ph_4C_4MMe)_nOMe$ (M = Si, $M_n = 5400$; Me = Ge, $M_n = 4400$), were prepared similarly from condensation of $Ph_4C_4MCl_2$ with Li followed by MeOH workup [74g]. Three polymer sets were prepared, one by the condensation of $Ph_4C_4SiLi_2$ and $Ph_4C_4GeCl_2$ giving $MeO(Ph_4C_4Si—GeC_4Ph_4)_nOMe$ ($M_n = 5000$) and two other types from the condensation of $Ph_4C_4MCl_2$ with $R^1R^2M'Cl_2$ that gave $MeO(Ph_4C_4Si—SiR^1R^2)_nOMe$ (five examples, $M_n = 4000$–4800) and $MeO(Ph_4C_4Ge—SiR^1R^2)_nOMe$ (four examples, $M_n = 3900$–5000). The degree of polymerization corresponded to 10–16 metallole units and the products should be considered as extended oligomers. The polysilole and the silole–silane copolymers have ~3–11-fold longer fluorescence lifetimes than the polygermole and germole–silane copolymers. The fluorescence lifetimes in thin films for the polysilane and polygermane are 2.5- and 4.2-fold longer than in toluene. The polymers functioned as sensors for nitroaromatics and each of the polymers exhibited a different ratio of PL quenching for picric acid, TNT, DNT, and nitrobenzene [74g]. The mechanism of PL quenching was attributed to electron transfer from the excited metallole to the LUMO of the analyte. TNT, with the less negative reduction potential of the analytes listed, was detected with the highest sensitivity. These polymers were not tested for the AIE effect.

In the following examples, the silole is incorporated into a polymer chain through the 2,5-positions. Chen and co-workers reported two sets of polymers that are loosely based on 2,3,4,5-tetraphenylsilole-containing polyfluorenes [74h,i]. The silole required for incorporation into the polymers was formed by the Tamao procedure. In one polymer set the intermediate, $Ph_2(ZnCl)_2C_4SiMe_2$, was cross-coupled with *p*-BrC_6H_4I [catalyst, $PdCl_2(PPh_3)_2$] to form $Ph_2(BrC_6H_4)_2C_4SiMe_2$ in 71% yield. The five PFO–PSP polymers reported were prepared by Pd^0 Suzuki coupling from equivalent molar ratios of the 2,7-diboronic ester and the 2,7-dibromo-substituted 9,9-dioctylfluorene with varying molar ratios of $Ph_2(C_6H_4Br)_2C_4SiMe_2$. The M_ws (GPC) ranged from 21 100 (fluorene:silole = 50:50) to 61 300 (fluorene:silole = 85:15). The Φ_{PL} of dilute THF solutions of the polymers ranged from 30% for PFO–PSP5 to 13% for PFO–PSP50 (Figure 1.5a) . The

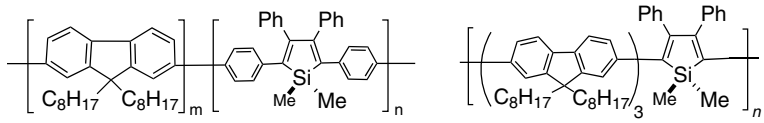

(a) M_w = 21 100, PFO-PSP50, 78% [74h] (b) M_w = 234 000, PF_3S, 87% [74i]

Figure 1.5 *Selected silole-containing polymers connected through 2,5-positions.*

quantum efficiencies measured for thin films varied from 55% (PFO–PSP50) to 84% (PFO–PSP10). The PSP portion of the polymer may be considered a tetraphenylsilole derivative and shows the AIE phenomenon [74h]. In the second set of polymers, the same Tamao intermediate, $Ph_2(ClZn)_2C_4SiMe_2$, was added by *reverse* addition to the 2,7-dibromo-9,9-dioctylfluorene to produce, in the presence of $PdCl_2(PPh_3)_2$, the silole with 2,5-bisfluorenyl substituents that also had Br substituents in the 7-position of the fluorene skeleton (BrFSFBr) [74i]. Thus, Suzuki coupling [$Pd(PPh_3)_4$] of the same 2,7-diboronic ester and BrFSFBr provided the alternating polymer $–[(Fl)_3–(Ph_2C_4SiMe_2)–]_n$, PF_3S (Figure 1.5b). With equimolar 2,7-diboronic ester and the 2,7-dibromo-substituted 9,9-dioctylfluorene and varying amounts of BrFSFBr, alternating copolymers were produced. The PL of films (integrating sphere) showed PF_3S to have the highest value (83%), 'reflecting the important aggregation-induced emission characteristics of siloles.' The four copolymers showed exclusive silole emissions, demonstrating that the silole units are efficient exciton traps [74i].

Tang and co-workers reviewed the AIE of siloles and polymers including their various applications [31c] and Chen and Cao included silole-containing polymers in a review of conjugated donor polymers for bulk-heterojunction photovoltaic devices [74j].

1.7.3 Polymers with silole pendants and hyperbranched polymers

In the previous section, the silole was part of the polymer chain. In this section, the silole is attached either directly as a substituent on a carbon atom of the chain or is attached to the carbon through a tether. Several of these were reported by Tang and co-workers in 2003 [75a–c] but only selected aspects are summarized here.

Polyacetylenes (PSA, poly(1,2,3,4,5-pentaphenylsilolylacetylene); PS9A, poly{11-[(1,2,3,4,5-pentaphenysilolyl)oxy]-1-undecyne}; PS9PA poly{11-[1,2,3,4,5-pentaphenylsilolyl)oxy}]-1-phenyl-1-undecyne}) were reported from polymerization of HC≡CPS, HC≡COPS, and $PhC{\equiv}C(CH_2)_9OPS$, respectively [75a–c]. The polymers were almost nonluminescent when molecularly dissolved but PS9A and PS9PA became emissive when aggregated in poor solvents (methanol–chloroform) or when cooled to temperatures lower than room temperature, thus demonstrating the AIE effect. Such behavior was not exhibited by PSA. For PS9A, Φ_{PL} rose from 0.15 to 2.95%, ~20-fold higher. For PS9PA, in 9:1 methanol–chloroform the value was 9.3% [75a]. Thus PS9PA was the most efficient emitter. The optical properties have been related to the molecular structure of the polymer. In PSA, direct electronic communication between the silole pendant and the polyacetylene backbone is possible, leading to better conjugation and efficient energy transfer from the silole to the main chain. However, the direct attachment of the silole to the rigid polymer backbone may prevent efficient packing of the silole groups in the aggregated state, therefore preventing the appearance of the AIE effect. Since the other two polymers are tethered to the polymer chain, the more isolated silole rings can then function as emitting centers in the polymer nanoaggregates, providing almost 46 times the enhancement over solution values. Overall, PSA emits from its polyacetylene backbone and PS9A from its silole pendants and PS9PA from both the backbone and the pendants, thus producing the best emitter. The emission resulting from cooling a solution sample [cooling-enhanced emission (CEE)] is attributed to

RIR of the phenyl groups with decreasing solution temperature, similar to what occurs in the formation of the aggregates in poor solvents [75b,c]. A fourth polymer, PS3DPA [Ph_4C_4SiMeX, X = –OC_6H_4–$O(CH_2)_3$–C≡C–PS] was described in 2004 and 2006, although it is not AIE active in poor solvents but does exhibit CEE [75d,e]. PS9A and PS9PA were the first examples of AIE-active polymers that exhibited silole-dominant emissions when aggregates of the polymers formed. A study of the time-resolved fluorescence and fluorescent lifetimes of the aggregate state provided direct evidence for the restricted molecular motion proposal as an explanation of the AIE effect in aggregates or the solid state [75f]. Polymers with silole pendants were included as examples of luminogenic polymers with AIE characteristics in a review by Tang and co-workers, and the review also included the hyperbranched polymers described in the next paragraph [75g,h].

Hyperbranched polymers, poly(phenylenesilolene)s, were generated from $Ph_4C_4Si(C{\equiv}CH)_2$ and HC≡CR (R = hexyl) in four different feed ratios catalyzed by $TaCl_5$—$SnPh_4$ [75a,c,d]. The hyperbranched polymers were weakly luminescent in THF with $\Phi_F \approx 1\%$ (compared with low molecular weight siloles at 0.1%) and are AIE inactive in MeOH—$CHCl_3$. However, when a dioxane solution of the hyperbranched polymer is cooled below room temperature the PL increases (an example of CEE) [75c]. A similar effect is observed at a slower rate on cooling THF solutions. The enhanced emission on cooling of solutions is attributed to restriction of intramolecular rotations by cooling. The hyperbranched polymers have nonlinear optically active properties and attenuate the optical power of laser pulses better than does C_{60}, a known optical limiter [75a,c,d].

1.7.4 Polybenzosiloles and ladder polymers

Several examples of conjugated molecules that contain multiple benzosilole units derived from 3-stannylbenzosilole that were transmetallated to a zinc intermediate and then cross-coupled with various aromatic dihalides to give benzosilole-substituted aromatic systems have been reported and included cross-coupling of an aromatic trichloride. From the crystal structure of the *p*-bis(dibenzosilole)benzene example, it appears that the 3-substituent forces the 2-substituent out of the benzosilole plane. The benzosiloles were utilized as hole-blocking materials for phosphorescent OLEDs with EQE values ranging from 3.3 to 5.8% [71e].

In another study, a diarylalkyne containing an *o*-(EtO)R_2Si-substituted aryl group with an additional OMe or F substituent *para* to the Si center was reductively coupled with LiNaph, followed by treatment with I_2 to give substituted bis-silicon-bridged stilbenes (disilaindeno[2,1-*a*]indene) [76a,b]. Subsequent treatment with ^{s}BuLi followed by I_2 or ^{i}PrOB(pin) gave the silicon-bridged stilbenes with I or B(pin) *meta* to the Si center. In the case where F was *para* to the Si, Li^{t}Bu_2Zn · TMP was used followed by I_2 and Suzuki–Miyama coupling of the iodide with ^{i}PrOB(pin), which produced the boron substituent in the F counterpart. Various cross-coupling methodologies that utilized Pd catalysts provided homopolymers (two examples) and heteropolymers (three polymers). The fluorescence properties of these copolymers are highly dependent on the nature of the combined comonomer units. The Φ_F values in THF for the two homopolymers were 36 and 63% and that of the heteropolymer with two different disilastilbene units was 51%. These three polymers exhibited intense blue to greenish blue fluorescence. The quantum yields increased with increasing ratio of fluoro-substituted stilbene, The heteropolymers with dialkynyl or dithiophene linkers at the 2,7-positions exhibited green and orange emission colors, respectively, and have lower Φ_F values [76a,b]. These polymers also were not tested for an AIE property.

Yamaguchi and co-workers also reported another set of ladder polymers, oligo(*p*-phenylenevinylene)s (LOPVs), with silicon and carbon bridges [76c,d]. Two types of cyclization reactions are required: an intramolecular reductive cyclization followed by a Friedel–Crafts cyclization. Two starting materials, 1,4-bis(phenylethynyl)benzenes, were used, one of which had *o*-HMe_2Si– groups on the terminal phenyl groups and the other HMe_2Si– groups on the central benzene ring. The reductive cyclization involved treatment

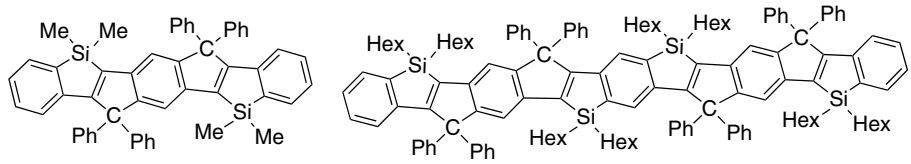

Figure 1.6 *Selected ladder polymers.*

with LiNaph followed by quenching with Ph_2CO, forming a diol, and the second step involved electrophilic cyclization of the alcohol that was initiated by $BF_3{\cdot}OEt_2$ and which generated the seven-ring ladder system with terminal silaindene rings from the former and the isomer of the seven-ring ladder (Figure 1.6a) with terminal indene rings. The related 9-, 11-, and 13-ring ladders (Figure 1.6b) were also reported. All the ladder polymers exhibit intense fluorescence in the visible region. The extension of the π-conjugation from the 9 to 11 to 13 fused rings red shifts the emission maxima by $\sim$80 nm (in THF) with a change in Φ_F from 84 to 40 to 59% in the series. The emission colors vary from blue (9-ring) to green (11-ring) to yellow (13-ring). The incorporation of Si provides σ^*–π^* conjugation that lowers the LUMO and leads to a red shift in the absorption and decreases the oscillator strength of the π^*–π^* transition resulting in the suppression of the radiative pathway from the excited singlet state [76d]. The ladder polymers were not tested for an AIE property.

1.7.5 Polymers that contain silafluorenes

Silafluorenes in polymers have been featured in three reviews. In a review that focused on the search for renewable sources of energy, the bridged phenylenes poly(2,7-fluorene), poly(2,7-carbazole), and poly(2,7-dibenzosilole) incorporated into photovoltaic devices and white light-emitting diodes were discussed [77a]. Silafluorenes as materials for organic electronics have also been reviewed by Wong *et al.* [77b]. An additional review by Tang and co-workers on AIE in silole molecules also contains material on polymers [31c].

Three soluble semiconducting silafluorene polymers were reported by Marks and co-workers [77c] from a synthetic protocol that started with 2,5-dibromonitrobenzene and in four steps provided the appropriate 2,7-dibromo-9,9′-di-*n*-octyldibenzosilole, which was also the source of the related 2,7-bis(4,4,5,5-tetramethyl-1,3,2-dioxaborolan-2-yl)-substituted silafluorene. Suzuki coupling of the dibromosilafluorene and the dioxaborolan-2-ylsilafluorene provided the homopolymer (BS8; Figure 1.7a) and coupling of the dibromosilafluorene with dioxaborolan-2-ylthiophene and bithiophene produced two copolymers [BS8T1 (Figure 1.7b) and BS8T2, respectively]. A set of silole–thiophene polymers was also reported and fluorene–

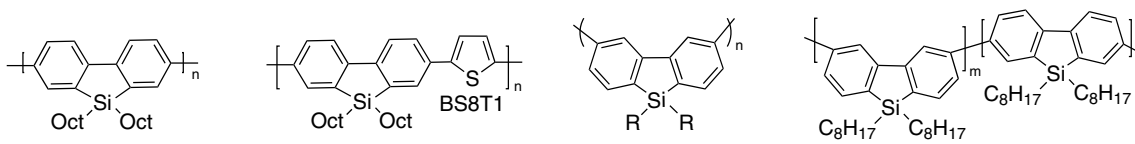

(a) BS8, Suzuki coupling M_w = 32 kDa, 76% [77c]
(b) BS8T1, Suzuki coupling M_w = 112 kDa, 60% [77c]
(c) R = C_6H_{13} (PSiFC_6C_6) M_w = 16 000 [77e,f]
(d) P36-27SiF90 M_w = 47 000, 70% [77g]

Figure 1.7 *Selected polymers that contain silafluorene.*

thiophene copolymers were prepared for comparison with both sets of polymers. The polymers were incorporated into devices in air and although BS8 exhibited no FET (field-effect transistor) activity, the other polymers were p-channel OTFTs (organic thin-film transistors). DFT calculations demonstrated that the presence of Si heteroatoms in both the silafluorene and dithienosilole cores provided a greater O_2 stability than the carbon analogs. An important aspect of this paper was the discussion of the processing methodology and the various efforts that were made to improve performance. A homopolymer equivalent to BS8 but with hexyl substituents on the Si center was also reported by Holmes and co-workers [77d].

The rarer substitution pattern from coupling at the 3,6-positions of a silafluorene also produced a wide-gap conjugated polymer (PSiFC6C6; Figure 1.7c) [77e]. The 3,6-dichloro-9,9′-alkylsilafluorene (two examples) employed to generate the polymer was prepared in four steps from 2,2′-dibromobiphenyl and was then coupled with the combination $NiCl_2$–PPh_3–2,2′-bipyridyl–Zn in dimethylacetamide. The coupling of chloride substituents is relatively rare in silafluorene systems [77e]. The PSiFC6C6 polymer served as a host for a blue iridium(III) complex and the combination produced a highly efficient blue light with a QE_{max} equal to 4.8% [77f]. In an additional publication, Cao and co-workers combined a 3,6-silafluorene (25%) and a 2,7-silafluorene through Suzuki coupling to give a blue-emitting polymer (Figure 1.7d) [77g]. The incorporation of the 3,6-silafluorene into poly(2,7-silafluorene) in the fabricated LED improved the color purity of the device and also the device efficiency (external quantum efficiency = 1.95%) [77g].

Polymers where the linking is through vinylene groups at a silicon center have also been prepared by Trogler and co-workers from the hydrosilylation of 9,9-dialkynylsilafluorene with 1,1-dihydrido(tetraphenylsilole) and with 9,9-dihydridosilafluorene, both of which were catalyzed by H_2PtCl_6. Solid-state PL data were obtained from spin-casting toluene solutions of the polymers on to quartz discs and by absorption of the polymer (in $CHCl_3$) spotted on silica gel TLC plates. In general, the TLC method [19] is more convenient and has good reproducibility, although in this case all the silafluorene–vinylene polymers exhibited a bathochromic shift from solution to TLC to quartz substrates. The polymers were used for the detection of nitroaromatic explosives by solution-phase fluorescence quenching of the polymers [74c]. In a second set of polymers, the dihydrosilafluorene was used to hydrosilylate 2,7-diethynyl-9*H*-fluorenes with various substituents at the 9-position (R, R′ = H, H; Me, Me; 9,9′-spirobifluorene) [77h]. The copolymer with the spirobifluorene exhibited the highest fluorescent quantum yield of 100% (thin film on quartz). The quartz plate may allow for the best ordering between the polymer chains in the deposit after evaporation. These polymers were also studied as chemosensors for explosives detection. Toal and Trogler published a short review of polymer sensors for nitroaromatic explosives detection in 2006 [77i].

1.7.6 Germoles in oligomers and polymers

There are few reports of germoles in polymers and the different types are included together in this section. Oligometalloles (estimated 10–16 units) that contained germoles were briefly included earlier in Section 1.7.2 [74g].

One of the earliest examples of oligogermoles appeared in 2000, predating the recognition of the AIE effect [78a]. Tilley and co-workers utilized the reaction of a tethered diyne with $Cp_2Zr(pyr)$ ($Me_3SiC{\equiv}CSiMe_3$) to obtain a zirconacycle followed by exchange with $GeBr_4$ to give the germole dibromide (Figure 1.8a). Since the tethered diyne contained terminal *p*-C_6H_4X (X = Cl or Br) groups, the germole that was formed incorporated these aryl groups in the 2,5-positions. Reaction of the germole dibromide with MeLi provided the germole with exocyclic Me substituents (a one-pot procedure with X = Cl gave a 61% yield and with X = Br an 88% yield). It is noteworthy that the alternative, using transmetallation with $GeCl_4$ or Me_2GeBr_2, gave lower yields. The freshly prepared monomer gave better results in polymerization reactions that utilized the catalyst system $NiCl_2$/Zn/PPh_3 in dimethylacetamide for the chlorophenyl substituents and the best results with this catalyst system were obtained with activated Zn and rigorously

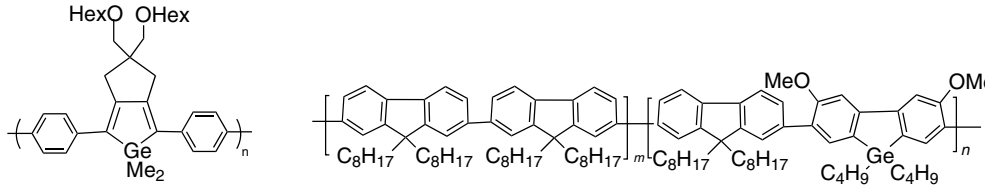

(a) M_n = 20 000, 90% [78a]

(b) PFO-DBuGeF-10
M_w = 34 900, 75% [78c]

Figure 1.8 *Example germole polymers.*

anhydrous conditions. A more efficient coupling system was obtained with $Ni(cod)_2$/bipyridine in toluene–DMF and the dibromide precursor. The three polymers reported had M_n values (by GPC) of 1900 and 4700 (from X = Cl; estimated degree of polymerization ~7 or 21 rings) and 20 000 (from X = Br). The shift in absorption maxima relative to the starting monomer indicated that the conjugation length of the polymer was longer than seven repeat units [78a]. These germole-containing polymers were the first to be reported utilizing the zirconocene exchange route to prepare the monomer precursors.

Hyperbranched poly(phenylenegermolene)s were prepared in the same way as the silicon analogs (Section 1.7.1) from the reaction of $Ph_4C_4Ge(C{\equiv}CH)_2$ (alone) or with HC≡CR (R = hex) catalyzed with $TaCl_5$–$SnPh_4$ [78b]. The homopolymer from the germole (47%, $M_w = 5160$) is soluble in common solvents. The copolymer produced from the germole and HC≡CR gave $M_w = 4450$ and also a soluble and processable heteropolymer that was thermally stable. The emission of the homopolymer in 9:1 MeOH–THF is weaker than that exhibited in $CHCl_3$, indicating that the homopolymer is AIE inactive (as was the related silicon hyperbranched polymer). However, when THF solutions of the homopolymer are cooled, the PL intensity increases. The similarity of emission maxima at −196 °C suggests that the PL is related to the radiative decay of the singlet excitons and not the triplet species [78b].

The last study involved germafluorene–fluorene copolymers, which were prepared by Suzuki coupling from a mixture of 10 mol% 2,7-dibromo-3,6-dimethoxy-9,9-dibutyl-9-germafluorene, 40 mol% 9,9-dioctylfluorene-2,7-dibromide, and 50 mol% 9,9-dioctylfluorene-2,7-bis(trimethylene boronate) [78c]. The PFO–DBuGeF10 (PFO = fluorene units; DBUGeF = the germafluorene; Figure 1.8b) produced had an M_n of 21 800 (GPC) and a PDI (polydispersity index) of 1.60. The cross-coupling catalyst was $Pd(PPh_3)_4$/Aliquat 336/Na_2CO_3(aq.) and the polymer was end-capped with phenylboronic acid (75% yield). From the ^{1}H NMR signal of the OMe group, the content of germafluorene was determined as 10.6%, slightly higher than the feed content, which may indicate a higher copolymerization ability of the dibromogermafluorene precursor. The quantum efficiency of the cast films of PFO–DBuGeF10 was 70%. The optical properties of the polymer were stable in air to 150 °C but thermal oxidation occurred at 200 °C. From CV data, the germafluorene copolymer has a lower LUMO than the polysilafluorene, indicating a greater impact of a Ge center than an Si center. PFO–DBuGeF10 was the first germafluorene-containing conjugated copolymer to be prepared and incorporated into a PLED, and the resulting nonoptimized device exhibited a quantum efficiency of 8.5% [78c].

1.8 Summary and Future Directions

The synthesis of siloles and their related benzene-annulated systems have one preparative route in common, that is, the reaction of a dilithio reagent with a dichlorosilane (or related trichlorosilane or silicon tetrachloride). Although these are basically the oldest routes to these systems, they are still employed today. The

traditional route to siloles provides all phenyl substituents on the carbon core of the silole. A more modern route to siloles involves ring closure of a dialkynylsilane by reductive coupling of the terminal alkyne units with Li or LiNaph providing a silole with anionic carbons α to the silicon center that are normally quenched with $ZnCl_2$ and then cross-coupled to a variety of aryl bromides to provide substituents at the α-carbons (2,5-substituents) that differ from those at the β-carbon (3,4-substituents). It is the manipulation of the substituents at the 2,5-positions that has allowed siloles to be electronically tuned with a variety of both electron-withdrawing and electron-donating units and has led to an improvement in properties that are desirable as core components for electronic devices. The identification of the AIE effect exhibited by siloles has added new applications, for example, materials as chemical sensors, in biological probes and smart nanomaterials. The more recent effort in silafluorene systems prepared through the dilithiobiphenyl route has been the synthesis of more complex biphenyls with additional substitutents, particularly those that would be in 2,7- or 3,6-positions in the metallafluorene, as these are involved in the formation of polymers. The 2,7-positions may provide electronic tuning, as is the case for 2,5-substituted siloles.

The use of transition metal-catalyzed processes to initiate ring closure of an arylsilane with an alkyne or of ring closure between two aryl groups in $ArAr'SiX_2$ has been of relatively recent origin. These routes have allowed the preparation of metallaindenes and metallafluorenes with substitution patterns that are not found in the traditional routes to these systems. The compounds provided with this new chemistry include unsymmetrically substituted benzo ring carbons in metallafluorenes and metallaindenes with substituents on the benzo ring. The routes seem to be effective for both silicon and germanium heterocycles and allows the formation of D–π–A variations of metallafluorenes. The majority of the transition metal-mediated processes require the incorporation of aryl groups in the silicon (or germanium) precursor that would normally be done with aryllithium reagents (from an ArBr or ArI), which in turn must incorporate the desired additional substituents prior to bond formation at Si or Ge. Hence efficient organic chemical processes are required to generate the desired silicon and germanium heterocycles.

Many authors still do not test for the AIE effect in the newly prepared metalloles and related benzene-annulated systems that are prepared, even though such tests are relatively simple to execute. Also underreported are measurements of quantum efficiency in the solid state. This should change in the future as the search for new systems continues. In cases where devices containing metalloles and metallafluorenes were prepared and properties measured, generally only one or two configurations are described in a report and there does not seem to be an effort to maximize the performance of the device. There are exceptions to this observation, of course, including the study by Marks and co-workers [77c], and another example appeared in a recent report on silylene-bridged 2-(2-naphthyl)indole [79].

Germanium chemistry is not as developed as silicon chemistry and, although the two elements are closely related, the chemical transformations that are so useful in silicon chemistry often do not transfer to this heavier member of Group 14. The reasons for this are not often very clear but impact even on the coupling of organometallic reagents with Ge—Cl bonds. The lack of extension of the Tamao method to the synthesis of germoles is also a problem. Germoles and the related benzene-annulated systems do not appear to have been reviewed since 1990 [8a], although only selected aspects of a few publications were included in this chapter. There are a few indications that the germanium systems are more effective in terms of quantum efficiencies (primarily measured in solution) than their silicon counterparts, but there are, as yet, insufficient numbers of cases to generalize a trend. Considering the additional difficulties encountered in germanium chemistry and the expense of the precursors, the development of germoles and germafluorenes for electronic devices is bound to lag behind that of the silicon counterparts. Some of the more interesting silicon systems that have not been covered in this brief chapter include dithienosiloles, fused-ring ladder oligomers and derivatives related to silafluorene such as silicon-bridged benzene–heteroarenes. Work in these areas and also the siloles and silafluorenes continues to evolve and produce better examples as components in electronic devices, and this trend can be expected to continue into the future.

References

1. Luo, J., Xie, Z., Lam, J.W.Y., Cheng, L., Chen, H., Qiu, C., Kwok, H.S., Zhan, X., Liu, Y., Zhu, D., and Tang, B.Z. (2001) *Chem. Commun.*, 1740–1741.
2. Tamao, K., Uchida, M., Izumizawa, T., Furukawa, K., and Yamaguchi, S. (1996) *J. Am. Chem. Soc.*, **118**, 11974–11975.
3. (a) Braye, E.H., and Hübel, W. (1959) *Chem. Ind. (London)*, 1250; *Chem. Abstr.*, 1960, **54**, 4538h; (b) Braye, E.H., Hübel, W., and Caplier, I. (1961) *J. Am. Chem. Soc.*, **83**, 4406–4410.
4. Tamao, K., and Yamaguchi, S. (1996) *Pure Appl. Chem.*, **68**, 139–144.
5. Zhan, X., Barlow, S., and Marder, S.R. (2009) *Chem. Commun.*, 1948–1955.
6. Yamaguchi, S., and Tamao, K. (2005) *Chem. Lett.*, **34**, 2.
7. (a) Corey, J.Y. (1975) *Adv. Organomet. Chem.*, **13**, 139–271; (b) Hermanns, J., and Schmidt, B. (1998) *J. Chem. Soc., Perkin Trans.* **1**, 2209–2230; (c) Hermanns, J., and Schmidt, B. (1999) *J. Chem. Soc., Perkin Trans.* **1**, 81–102.
8. (a) Dubac, J., Laporterie, A., and Manuel, G. (1990) *Chem. Rev.*, **90**, 215–263, Armitage, D.A. (1996) *Comprehensive Heterocycl. Chem. II*, **2**, 903–918; (b) Dubac, J., Guerin, C., and Meunier, P. (1998) *Chem. Org. Silicon Compd.*, **2**(Pt. 3), 1961; (c) Corey, J.Y. (2011) *Adv. Organomet. Chem.*, **59**, 1–180.
9. (a) Smith, L.I., and Hoehn, H.H. (1941) *J. Am. Chem. Soc.*, **63**, 1184–1187; (b) Joo, W.-C., Park, Y.C., Kang, S.K., and Hong, J.H. (1987) *Bull. Korean Chem. Soc.*, **8**, 270; (c) Joo, W.-C., Hong, J.-H., Choi, S.-B., Son, H.-E., and Kim, C.H. (1990) *J. Organomet. Chem.*, **391**, 27–36.
10. Dong, Y., Lam, J.W.Y., Qin, J.-K., Sun, J.-Z., Dong, Y., and Tang, B.Z. (2007) *Chem. Phys. Lett.*, **446**, 124–127.
11. Zhan, X., Risko, C., Amy, F., Chan, C., Zhao, W., Barlow, S., Kahn, A., Brédas, J.-L., and Marder, S.R. (2005) *J. Am. Chem. Soc.*, **127**, 9021–9029.
12. Zhan, X., Haldi, A., Risko, C., Chan, C.K., Zhao, W., Timofeeva, T.V., Korlynukov, A., Antipin, M.Y., Montgomery, S., Thompson, E., An, Z.S., Domercq, B., Barlow, S., Kahn, A., Kippelen, B., Brédas, J.-L., and Marder, S.R. (2008) *J. Mater. Chem.*, **18**, 3157–3166.
13. Li, Z., Dong, Y., Mi, B., Tang, Y., Häussler, M., Tong, H., Dong, Y., Lam, J.W.Y., Ren, Y., Sung, H.H.Y., Wong, K.S., Gao, P., Williams, I.D., Kwok, H.S., and Tang, B.Z. (2005) *J. Phys. Chem. B*, **109**, 10061–10066.
14. Yin, S., Peng, Q., Shuai, Z., Fang, W., Wang, Y.-H., and Luo, Y. (2006) *Phys. Rev. B*, **73**, 205409.
15. Luo, J., Xie, Z., Lam, J.W.Y., Cheng, L., Chen, H., Qiu, C., Kwok, H.S., Zhan, X., Liu, Y., Zhu, D., and Tang, B.Z. (2001) *Chem. Commun.*, 1740–1741.
16. Tang, B.Z., Zhan, X., Yu, G., Lee, P.P.S., Liu, Y., and Zhu, D. (2001) *J. Mater. Chem.*, **11**, 2974–2978.
17. Ferman, J., Kakareka, J.P., Klooster, W.T., Mullin, J.L., Quattrucci, J., Ricci, J.S., Tracy, H.J., Vining, W.J., and Wallace, S. (1999) *Inorg. Chem.*, **38**, 2464–2472.
18. He, G., Peng, H., Liu, T., Yang, M., Zhang, Y., and Fang, Y. (2009) *J. Mater. Chem.*, **19**, 7347–7353.
19. Chen, J., Law, C.C.W., Lam, J.W.Y., Dong, Y., Lo, S.M.F., Williams, I.D., Zhu, D., and Tang, B.Z. (2003) *Chem. Mater.*, **15**, 1535–1546.
20. Tracy, H.J., Mullin, J.L., Klooster, W.T., Martin, J.A., Haug, S.W., Rudloe, I., and Watts, K. (2005) *Inorg. Chem.*, **44**, 2003–2011 (X-ray data are in the supplemental material).
21. Zhan, X., Risko, C., Amy, F., Chan, C., Zhao, W., Barlow, S., Kahn, A., Brédas, J.-L., and Marder, S.R. (2005) *J. Am. Chem. Soc.*, **127**, 9021–9029.
22. Sun, Y., Li, Y., Chen, Y., and Ma, F. (2006) *J. Mol. Struct.: THEOCHEM*, **770**, 51–56.
23. Yin, S., Yi, Y., Li, Q., Yu, G., Liu, Y., and Shuai, Z. (2006) *J. Phys. Chem. A*, **110**, 7138–7143.
24. Yu, G., Yin, S., Liu, Y., Chen, J., Xu, X., Sun, X., Ma, D., Zhan, X., Peng, Q., Shuai, Z., Tang, B., Xhu, D., Fang, W., and Luo, Y. (2005) *J. Am. Chem. Soc.*, **127**, 6335–6346.
25. Heng, L., Zhai, J., Qin, A., Zhang, Y., Dong, Y., Tang, B.Z., and Jiang, L. (2007) *ChemPhysChem*, **8**, 1513–1518.
26. Chan, C.P.-y., Haeussler, M., Tang, B.Z., Dong, Y., Sin, K.-k., Mak, W.-C., Trau, D., Seydack, M., and Renneberg, R. (2004) *J. Immunol. Methods*, **295**, 111–118.
27. Bhongale, C.J., Chang, C.-W., Diau, E. W.-G., Hsu, C.-S., Dong, Y., and Tang, B.-Z. (2006) *Chem. Phys. Lett.*, **419**, 444–449.

28. Dong, Y., Lam, J.W.Y., Li, Z., Qin, A., Tong, H., Dong, Y., Feng, X., and Tang, B.Z. (2005) *J. Inorg. Organomet. Polym. Mater.*, **15**, 287–291.
29. Heng, L., Dong, Y., Zhai, J., Tang, B., and Jiang, L. (2008) *Langmuir*, **24**, 2157–2161.
30. Chen, J., Xu, B., Yang, K., Cao, Y., Sung, H.H.Y., Williams, I.D., and Tang, B.Z. (2005) *J. Phys. Chem. B*, **109**, 17086–17093.
31. (a) Hong, Y., Lam, J.W.Y., and Tang, B.Z. (2011) *Chem. Soc. Rev.*, **40**, 5361–5388; (b) Hong, Y., Lam, J.W.Y., and Tang, B.Z. (2009) *Chem. Commun.*, 4332–4353; (c) Liu, J., Lam, J.W.Y., and Tang, B.Z. (2009) *J. Inorg. Organomet. Polym.*, **19**, 249–285.
32. Yamaguchi, S., and Tamao, K. (1998) *J. Chem. Soc., Dalton Trans.*, 3693–3702.
33. Yamaguchi, S., and Tamao, K. (2002) *J. Organomet. Chem.*, **653**, 223–228.
34. (a) Tamao, K., Yamaguchi, S., and Shiro, M. (1994) *J. Am. Chem. Soc.*, **116**, 11715–11722; (b) Yamaguchi, S., Endo, T., Uchida, M., Izumizawa, T., Furukawa, K., and Tamao, K. (2000) *Chem. Eur. J.*, **6**, 1683–1692.
35. Lee, J., Liu, Q.-D., Bai, D.-R., Kang, Y., Tao, Y., and Wang, S. (2004) *Organometallics*, **23**, 6205–6213.
36. Boydston, A.J., and Pagenkopf, B.L. (2004) *Angew. Chem. Int. Ed.*, **43**, 6336–6338.
37. Zhao, Z., Liu, D., Mahtab, F., Xin, L., Shen, Z., Yu, Y., Chan, C.Y.K., Lu, P., Lam, J.W.Y., Sung, H.H.Y., Williams., I.D., Yang, B., Ma, Y., and Tang, B.Z. (2011) *Chem. Eur. J.*, **17**, 5998–6008.
38. Morra, N.A., and Pagenkopf, B.L. (2008) *Org. Synth.*, **85**, 53–63.
39. Boydston, A.J., Yin, Y., and Pagenkopf, B.L. (2004) *J. Am. Chem. Soc.*, **126**, 3724–3725.
40. Yamaguchi, S., Jin, R.-Z., and Tamao, K. (1997) *Organometallics*, **16**, 2230–2232.
41. (a) Zhan, X., Risko, C., Korlyukov, Sena, F., Timofeeva, T.V., Antipin, M.Y., Barlow, S., Brédas, J.-L., and Marder, S.R. (2006) *J. Mater. Chem.*, **16**, 3814–3822; (b) Booker, C., Wang, X., Haroun, S., Zhou, J., Jennings, M., Pagenkopf, B.L., and Ding, Z. (2008) *Angew. Chem. Int. Ed.*, **47**, 7731–7735; (c) Son, H.-J., Han, W.-S., Wee, K. R., Lee, S.-H., Hwang, A.-R., Kwon, S., Cho, D.W., Suh, I.-H., and Kang, S.O. (2009) *J. Mater. Chem.*, **19**, 8964–8973; (d) Palilis, L.C., Murata, H., Uchida, M., and Kafafi, Z.H. (2003) *Org. Electron.*, **4**, 113–121; (e) Lee, J., Liu, Q.-D., Motala, M., Dane, J., Gao, J., Kang, Y., and Wang, S. (2004) *Chem. Mater.*, **16**, 1869–1877; (f) Aubouy, L., Huby, N., Hirsch, L., van der Lee, A., and Gerbier, P. (2009) *New J. Chem.*, **33**, 1290–1300.
42. Zhao, Z., Wang, Z., Lu, P., Chan, C.Y.K., Liu, D., Lam, J.W.Y., Sung, H.H.Y., Williams, I.D., Ma, Y., and Tang, B.Z. (2009) *Angew. Chem. Int. Ed.*, **48**, 7608–7611.
43. Zhao, Z., Liu, D., Mahtab, F., Xin, L., Shen, Z., Yu, Y., Chan, C.Y.K., Lu, P., Lam, J.W.Y., Sung, H.H.Y., Williams, I.D., Yang, B., Ma, Y., and Tang, B.Z. (2011) *Chem. Eur. J.*, **17**, 5998–6008.
44. Ding, C., Babu, G., Orita, A., Hirate, T., and Otera, J. (2007) *Synlett*, **16**, 2559–2563.
45. Li, S., Leng, T., Zhong, H., Wang, C., and Shen, Y. (2012) *J. Heterocycl. Chem.*, **49**, 64–70.
46. Bozeman, T.C., Edwards, K.A., Fecteau, K.M., Verde, M.G., Jr, Blanchard, A., Woodall, D.L., Benfaremo, N., Ford, J.R., Mullin, J.L., Prudente, C.K., and Tracy, H.J. (2011) *J. Inorg. Organomet. Polym. Mater.*, **21**, 316–326.
47. (a) Son, H.-J., Han, W.-S., Wee, K.R., Lee, S.-H., Hwang, A.-R., Kwon, S., Cho, D.W., Suh, I.-H., and Kang, S.O. (2009) *J. Mater. Chem.*, **19**, 8964–8973; (b) Lee, H., Kim, J., and Kang, Y. (2007) *Inorg. Chem. Commun.*, **10**, 731–734.
48. Mei, J., Wang, J., Sun, J.Z., Zhao, H., Yuan, W., Deng, C., Chen, S., Sung, H.H.Y., Lu, P., Qin, A., Kwok, H.S., Ma, Y., Williams, I.D., and Tang, B.Z. (2012) *Chem. Sci.*, **3**, 549–558.
49. (a) Zhao, Z., Guo, Y., Jiang, T., Chang, Z., Lam, J.W.Y., Xu, L., Qiu, H., and Tang, B.Z. (2012) *Macromol. Rapid Commun.*, **33**, 1074–1079; (b) Zhao, Z., Chen, S., Shen, X., Mahtab, F., Yu, Y., Lu, P., Lam, J.W.Y., Kwok, H.S., and Tang, B.Z. (2010) *Chem. Commun.*, **46**, 686–688; (c) Zhao, Z., Chen, S., Lu, P., Deng, C., Kwok, H.S., Ma, Y., and Tang, B.Z. (2010) *J. Phys. Chem. C.*, **114**, 7963–7972.
50. Köster, R., Seidel, G., Süss, J., and Wrackmeyer, B. (1993) *Chem. Ber.*, **126**, 1107.
51. Wrackmeyer, *B. Coord. Chem. Rev.* (1995) **145**, 125–156.
52. Selected examples: (a) Wrackmeyer, B., Bhatti, M.H., Ali, S., Tok, O.L., and Bubnov, Y.N. (2002) *J. Organomet. Chem.*, **657**, 146–154; (b) Wrackmeyer, B., Milius, W., Klimkina, E.V., and Bubnov, Y.N. (2001) *Chem. Eur. J.*, **7**, 775–782; (c) Wrackmeyer, B., Tok, O.L., Shahid, K., and Ali, S. (2004) *Inorg. Chim. Acta*, **357**, 1103–1110; (d) Khan, E., Bayer, S., and Wrackmeyer, B. (2009) *Z. Naturforsch.*, **64B**, 995–1002; (e) Khan, E., Bayer, S., Kempe, R., and Wrackmeyer, B. (2009) *Eur. J. Inorg. Chem.*, 4416–4424; (f) Wrackmeyer, B., Kehr, G., Süss, J., and Molla, E. (1998) *J. Organomet. Chem.*, **562**, 207–215; (g) Wrackmeyer, B., Tok, O.L., Klimkina, E.V., and Milius, W. (2010) *Eur. J. Inorg. Chem.*, 2276–2282.

53. Khan, E., Wrackmeyer, B., and Kempe, R. (2008) *Eur. J. Inorg. Chem.*, 5367–5372.
54. (a) Dierker, G., Ugolotti, J., Kehr, G., Fröhlich, R., and Erker, G. (2009) *Adv. Synth. Catal.*, **351**, 1080–1088; (b) Ugolotti, J., Kehr, G., Fröhlich, R., and Erker, G. (2010) *Chem. Commun.*, 3016–3018; (c) Ugolotti, J., Dierker, G., Fröhlich, R., Kehr, G., and Erker, G. (2011) *J. Organomet. Chem.*, **696**, 1184–1188; (d) Möbus, J., Bonnin, Q., Ueda, K., Fröhlich, R., Itami, K., Kehr, G., and Erker, G. (2012) *Angew. Chem. Int. Ed.*, **51**, 1954–1957.
55. (a) Negishi, E., Cederbaum, F.E., and Takahashi, T. (1986) *Tetrahedron Lett.*, **27**, 2829; (b) Freeman, W.P., Tilley, T.D., Liable-Sands, L.M., and Rheingold, A.L. (1996) *J. Am. Chem. Soc.*, **118**, 10457–10468; (c) Hudrlik, P.F., Dai, D., and Hudrlik, A.M. (2006) *J. Organomet. Chem.*, **691**, 1257–1264; (d) Yamaguchi, S., Jin, R.-Z., and Tamao, K. (1998) *J. Organomet. Chem.*, **559**, 73–80; (e) Buchwald, S.L., and Nielsen, R.B. (1989) *J. Am. Chem. Soc.*, **111**, 2870–2874; (f) Xi, C., Huo, S., Afifi, T.H., Hara, R., and Takahashi, T. (1997) *Tetrahedron Lett.*, **38**, 4099–4102.
56. Liu, J., Zhang, W.-X., Guo, X., Hou, Z., and Xi, Z. (2007) *Organometallics*, **26**, 6812–6820.
57. (a) Xi, Z., and Zhang, W.-X. (2008) *Synlett*, **17**, 2557; (b) Xi, Z. (2010) *Acc. Chem. Res.*, **43**, 1342–1351.
58. Yamaguchi, S., Jin, R.-Z., Tamao, K., and Sato, F. (1998) *J. Org. Chem.*, **63**, 10060–10062.
59. (a) Fagan, P.J., and Nugent, W.A. (1988) *J. Am. Chem. Soc.*, **110**, 2310–2312; (b) Fagan, P.J., Nugent, W.A., and Calabrese, J.C. (1994) *J. Am. Chem. Soc.*, **116**, 1880–1889; (c) Kanno, K.-i., and Kira, M. (1999) *Chem. Lett.*, 1127–1128.
60. (a) Okinoshima, H., Yamamoto, K., and Kumada, M. (1972) *J. Am. Chem. Soc.*, **94**, 9263–9264; (b) Sanji, T., Ishiwata, H., Kaizuka, T., Tanaka, M., Sakurai, S., Nagahata, R., and Takeuchi, K. (2005) *Chem. Lett.*, **34**, 1130–1131; (c) Sanji, T., Ishiwata, H., Kaizuka, T., Tanaka, M., Sakurai, H., Nagahata, R., and Takeuchi, K. (2005) *Can. J. Chem.*, **83**, 646–651; (d) Sanji, T., Kanzawa, T., and Tanaka, M. (2007) *J. Organomet. Chem.*, **692**, 5053–5059; (e) Yamaguchi, S., Itami, Y., and Tamao, K. (1998) *Organometallics*, **17**, 4910–4916; (f) Matsuda, T., Suda, Y., and Fujisaki, Y. (2011) *Synlett*, 813–816; (g) Tang, B.Z., Xhan, X., Yu, G., Lee, P.P.S., Liu, Y., and Zhu, D. (2001) *J. Mater. Chem.*, **11**, 2974–2978.
61. (a) Ohmura, T., Masuda, K., and Suginome, M. (2008) *J. Am. Chem. Soc.*, **130**, 1526–1527; (b) Ohmura, T., Masuda, K., Takase, I., and Suginome, M. (2009) *J. Am. Chem. Soc.*, **131**, 16624–16625.
62. (a) Matsuda, T., Kadowaki, S., and Murakami, M. (2007) *Chem. Commun.*, 2627–2629; (b) Katkevics, M., Yamaguchi, S., Toshimitsu, A., and Tamao, K. (1998) *Organometallics*, **17**, 5796–5800.
63. (a) Toal, S.J., Jones, K.A., Magde, D., and Trogler, W.C. (2005) *J. Am. Chem. Soc.*, **127**, 11661–11665; (b) Wang, M., Zhang, D., Zhang, G., Tang, Y., Wang, S., and Zhu, D. (2008) *Anal. Chem.*, **80**, 6443–6448.
64. (a) Yamaguchi, S., Jin, R.-Z., Ohno, S., and Tamao, K. (1998) *Organometallics*, **17**, 5133–5138; (b) Yamaguchi, S., Jin, R.-Z., and Tamao, K. (1998) *J. Organomet. Chem.*, **559**, 73–80.
65. (a) Leavitt, F.C., Manuel, T.A., and Johnson, F. (1959) *J. Am. Chem. Soc.*, **81**, 3163–3164; (b) Leavitt, F.C., Manuel, T.A., Johnson, F., Matternas, L.U., and Lehman, D.S. (1960) *J. Am. Chem. Soc.*, **82**, 5099–5102; (c) Hota, N.K., and Willis, C.J. (1968) *J. Organomet. Chem.*, **15**, 89–96; (d) Curtis, M.D. (1969) *J. Am. Chem. Soc.*, **91**, 6011–6018; (e) West, R., Sohn, H., Powell, D.R., Mueller, T., and Apeloig, K. (1996) *Angew. Chem. Int. Ed.*, **35**, 1002–1004; (f) Ferman, J., Kakareka, J.P., Klooster, W.T., Mullin, J.L., Quattrucci, J., Ricci, J.S., Tracy, H.J., Vining, W.J., and Wallace, S. (1999) *Inorg. Chem.*, **38**, 2464–2472; (g) Curtis, M.D. (1967) *J. Am. Chem. Soc.*, **89**, 4241–4242; (h) Jutzi, R., and Karl, A. (1981) *J. Organomet. Chem.*, **215**, 19–25; (i) Lalov, A.V., Nasov, K.S., Egorov, M.P., and Nefedov, O.M. (2004) *Russ. Chem. Bull. Int. Ed.*, **53**, 2334–2335; (j) Meier-Brocks, F., and Weiss, E. (1993) *J. Organomet. Chem.*, **453**, 33–45; (k) Bandrowsky, T.L., Carroll, J.B., and Braddock-Wilking, J. (2011) *Organometallics*, **30**, 3559–3569.
66. (a) Fagan, P.J., and Nugent, W.A. (1988) *J. Am. Chem. Soc.*, **110**, 2310–2312; (b) Fagan, P.J., Nugent, W.A., and Calabrese, J.C. (1994) *J. Am. Chem. Soc.*, **116**, 1880–1889; (c) Dufour, P., Dartiguenave, M., and Dartiguenave, Y. (1990) *J. Organomet. Chem.*, **384**, 61–69; (d) Dufour, P., Dubac, J., Dartiguenave, M., and Dartiguenave, Y. (1990) *Organometallics*, **9**, 3001–3003; (e) Nitschke, J.R., and Tilley, T.D. (2003) *J. Organomet. Chem.*, **666**, 15–22.
67. (a) Wrackmeyer, B. (1986) *J. Organomet. Chem.*, **310**, 151–160; (b) Köster, R., Seidel, G., Klopp, I., Krüger, C., Kehr, G., Suss, J., and Wrackmeyer, B. (1993) *Chem. Ber.*, **126**, 1385–1396; (c) Wrackmeyer, B., Pedall, A., Milius, W., Ali, S., and Ponomarev, S.V. (2001) *Main Group Met. Chem.*, **24**, 603–608; (d) Matsuda, T., Kadowaki, S., Yamaguchi, Y., and Murakami, M. (2010) *Org. Lett.*, **12**, 1056–1058; (e) Billeb, G., Brauer, H., Neumann, W.P., and Weisbeck, M. (1992) *Organometallics*, **11**, 2069–2074.

68. Mullin.L., Tracy, H.J., Ford, J.R., Keenan, S.R., and Fridman, F. (2007) *J. Inorg. Organomet. Polym. Mater.*, **17**, 201–213.
69. (a) Park, Y.H., Shin, Y.H., and Kim, Y. (2010) *J. Korean Phys. Soc.*, **57**, 1463–1466; (b) Park, Y.H., Kim, Y., and Sohn, H. (2011) *J. Korean Phys. Soc.*, **59**, 2318–2323; (c) Park, Y.H., Kim, Y., Sohn, H., and An, K.-S. (2012) *J. Phys. Org. Chem.*, **25**(3), 207–210.
70. Bandrowsky, T.L., Carroll, J.B., and Braddock-Wilking, J. (2011) *Organometallics*, **30**, 3559–3569.
71. (a) Corey, J.Y. (2011) *Adv. Organomet. Chem.*, **59**, 181–328; (b) Rausch, M.D., and Klemann, L.P. (1967) *J. Am. Chem. Soc.*, **89**, 5732–5733; (c) Rausch, M.D., Klemann, L.P., and Boon, W.H. (1985) *Synth. React. Inorg. Met.-Org. Chem.*, **15**, 923–943; (d) Illies, L., Tsuji, H., Sato, Y., and Nakamura, E. (2008) *J. Am. Chem. Soc.*, **130**, 4240–4241; (e) Ilies, L., Sato, Y., Mitsui, C., Hayato, T., and Nakamura, E. (2010) *Chem. Asian J.*, **5**(6), 1376–1381; (f) Kanj, A., Meunier, P., Gautheron, B., Dubac, J., and Daran, J.-C. (1993) *J. Organomet. Chem.*, **454**, 51–58; (g) Choi, S.-B., Boujouk, P., and Qin, K. (2000) *Organometallics*, **19**, 1806–1809; (h) Shirakawa, E., Masui, S., Narui, R., Watabe, R., Ikeda, D., and Hayashi, T. (2011) *Chem. Commun.*, **47**, 9714–9716; (i) Liang, Y., Geng, W., Wei, J., and Xi, Z. (2012) *Angew. Chem. Int. Ed.*, **51**, 1934–1937; (j) Matsuda, T., Yamaguchi, Y., Shigeno, M., Sato, S., and Murakami, M. (2011) *Chem. Commun.*, **47**, 8697–8699; (k) Matsuda, T., Yamaguchi, Y., Isida, N., and Murakami, M. (2010) *Synlett*, 2743–2746; (l) Kuznetsov, A., and Gevorgyan, V. (2012) *Org. Lett.*, **14**, 914–917; (m) Matsuda, T., Kadowaki, S., Yamaguchi, Y., and Murakami, M. (2010) *Org. Lett.*, **12**, 1056–1058; (n) Tobisu, M., Baba, K., and Chatani, N. (2011) *Org. Lett.*, **13**, 3282–3284.
72. (a) Gilman, H., and Gorsich, R. (1955) *J. Am. Chem. Soc.*, **77**, 6380–6381; (b) Albright, H., Pustai, E., Touloukhonova, I., Temple, N., and West, R. (2012) Presented at the 44th Silicon Symposium, Brock University, St. Catharines, Ontario, Canada, Abstract 29; (c) Chen, R.-F., Fan, Q.-L., Zheng, C., and Huang, W. (2006) *Org. Lett.*, **8**, 203–205; (d) Li, L., Xu, C., and Li, S. (2010) *Tetrahedron Lett.*, **51**, 622–624; (e) Allard, N., Aïch, R.B., Gendron, D., Boudreault, P.-L.T., Tessier, C., Alem, S., Tse, S.-C., Tao, Y., and Leclerc, M. (2010) *Macromolecules*, **43**, 2328–2333; (f) Yabusaki, Y., Ohshima, N., Kondo, H., Kusamoto, T., Yamanoi, Y., and Nishihara, H. (2010) *Chem. Eur. J.*, **16**, 5581–5585; (g) Ureshino, T., Yoshida, T., Kuninobu, Y., and Takai, K. (2010) *J. Am. Chem. Soc.*, **132**, 14324–14326.
73. (a) Shimizu, M., Mochida, K., and Hiyama, T. (2008) *Angew. Chem. Int. Ed.*, **47**, 9760–9764; (b) Shimizu, M., Mochida, K., Katoh, M., and Hiyama, T. (2010) *J. Phys. Chem. C*, **114**, 10004–10014; (c) Shimizu, M., and Hiyama, T. (2012) *Synlett*, **23**, 973–989; (d) Shintani, R., Otomo, H., Ota, K., and Hayashi, T. (2012) *J. Am. Chem. Soc.*, **134**, 7305–7308.
74. (a) Sohn, H., Huddleston, R.R., Powell, D.R., and West, R. (1999) *J. Am. Chem. Soc.*, **121**, 2935–2936; (b) Toal, S. J., Sohn, H., Zakarov, L.N., Kassel, W.S., Golen, J.A., Rheingold, A.L., and Trogler, W.C. (2005) *Organometallics*, **24**, 3081–3087; (c) Sanchez, J.C., DiPasquale, A.G., Rheingold, A.L., and Trogler, W.C. (2007) *Chem. Mater.*, **19**, 6459–6470; (d) Sanchez, J.C., Urbas, S.A., Toal, S.J., DiPasquale, A.G., Rheingold, A.L., and and Trogler, W.C. (2008) *Macromolecules*, **41**, 1237–1245; (e) Boydston, A.J., Yin, Y., and Pagenkopf, B.L. (2004) *J. Am. Chem. Soc.*, **126**, 10350–10354; (f) Jang, S., Kim, S.G., Jung, D., Kwon, H., Song, J., Cho, S., Ko, Y.C., and Sohn, H. (2006) *Bull. Korean Chem. Soc.*, **27**, 1965–1966; (g) Sohn, H., Sailor, M.J., Magde, D., and Trogler, W.C. (2003) *J. Am. Chem. Soc.*, **125**, 3821–3830; (h) Wang, F., Luo, J., Chen, J., Huang, F., and Cao, Y. (2005) *Polymer*, **46**, 8422–8429; (i) Liu, Z., Wang, L., Chen J., Wang, F., Ouyang, X., and Cao, Y. (2007) *J. Polym. Sci. Part A*, **45**, 756–767; (j) Chen, J., and Cao, Y. (2009) *Acc. Chem. Res.*, **42**, 1709–1718.
75. (a) Lam, J.W.Y., Chen, J., Law, C.C.W., Peng, H., Xie, Z., Cheuk, K.K., and Tang, B.Z. (2003) *Macromol. Symp.*, **196**, 289–300; (b) Chen, J., Xie, Z., Lam, J.W.Y., Law, C.C.W., and Tang, B.Z. (2003) *Macromolecules*, **36**, 1108–1117; (c) Chen, J., Peng, H., Law, C.C.W., Dong, Y., Lam, J.W.Y., Williams, I.D., and Tang, B.Z. (2003) *Macromolecules*, **36**, 4319–4327; (d) Häussler, M., Chen, J., Lam, J.W.Y., and Tang, B.Z. (2004) *J. Nonlinear Opt. Phys. Mater.*, **13**, 335–345; (e) Chen, J., Kwok, H.S., and Tang, B.Z. (2006) *J. Polym. Sci. Part A*, **44**, 2487–2498; (f) Ren, Y., Lam, J.W.Y., Dong, Y., Tang, B.Z., and Wong, K.S. (2005) *J. Phys. Chem. B*, **109**, 1135–1140; (g) Qin, A., Lam, J.W.Y., and Tang, B.Z. (2012) *Prog. Polym. Sci.*, **37**, 182–209; (h) Liu, J., Lam, J.W.Y., and Tang, B.Z. (2009) *J. Inorg. Organomet. Polym.*, **19**, 249–285.
76. (a) Yamaguchi, S., Xu, C., and Tamao, K. (2003) *J. Am.Chem. Soc.*, **125**, 13662–13663; (b) Xu, C., Yamada, H., Wakamiya, A., Yamaguchi, S., and Tamao, S. (2004) *Macromolecules*, **37**, 8978–8983; (c) Xu, C., Wakamiya, A., and Yamaguchi, S. (2005) *J. Am.Chem. Soc.*, **127**, 1638–1639; (d) Yamaguchi, S., Xu, C., Yamada, H., and Wakamiya, A. (2005) *J. Organomet. Chem.*, **690**, 5365–5377.

77. (a) Beaupré, S., Boudreault, P.-L., T., and Leclerc, M. (2010) *Adv. Mater.*, **22**, E6–E27; (b) Wong, W.W.H., Hooper, J.F., and Holmes, A.B. (2009) *Aust. J. Chem.*, **62**, 393–401; (c) Lu, G., Usta, H., Risko, C., Wang, L., Facchetti, A., Ratner, M.A., and Marks, T.J. (2008) *J. Am. Chem. Soc.*, **130**, 7670–7685; (d) Chan, K.L., McKieman, M.J., Towns, C.R., and Holmes, A.B. (2005) *J. Am. Chem. Soc.*, **127**, 7662–7663; (e) Mo, Y., Tian, R., Shi, W., and Cao, Y. (2005) *Chem. Commun.*, 4925–4926; (f) Zhang, X., Jiang, C., Mo, Y., Xu, Y., Shi, H., and Cao, Y. (2006) *Appl. Phys. Lett.*, **88**, 051116-1–051116-3; (g) Wang, E., Li, C., Peng, J., and Cao, Y. (2007) *J. Polym. Sci. Part A: Polym. Chem.*, **45**, 4941–4949; (h) Sanchez, J.C., and Trogler, W.C. (2008) *J. Mater. Chem.*, **18**, 3143–3156; (i) Toal, S.J., and Trogler, W.C. (2006) *J. Mater. Chem.*, **16**, 2871–2883.
78. (a) Lucht, B.L., Buretea, M.A., and Tilley, T.D. (2000) *Organometallics*, **19**, 3469–3475; (b) Law, C.C.W., Chen, J., Lam, J.W.Y., Peng, H., and Tang, B.Z. (2004) *J. Inorg. Organomet. Polym.*, **14**, 39–51; (c) Chen, R.F., Zhu, R., Zheng, C., Liu, S.J., Fan, Q.L., and Huang, W. (2009) *Sci. China Ser. B: Chem.*, **52**, 212–218.
79. Shimizu, M., Mochida, K., Asai, Y., Yamatani, A., Raki, R., Hiyama, T., Nagai, N., Yamagishi, H., and Furutani, H. (2012) *J. Mater. Chem.*, **22**, 4337–4342.